# Mathematical Analysis of Similarity Solutions for Modelling Injection of $CO_2$ into Aquifers

Master of Science Thesis in Applied Mathematics

Andreas Sandvin

Department of Mathematics
University of Bergen


June 1, 2007

# Preface

As I have finished my thesis, there are some people that deserves to be mentioned. First, I would like to thank my supervisor Jan M. Nordbotten, for always being enthusiastic and supportive. I am grateful for all the help and guidance through the time on the master. I would also like to thank my co-supervisor Helge Dahle for many helpful and instructive advices, specially in these finishing weeks of my thesis. Further, I thank my good friend and fellow student Eirik Keilegavlen, for giving me helpful remarks on the writing of this thesis. For the rest of my fellow students, I thank you for two good years. At last, I thank my family for always being supportive.

Andreas Sandvin
Bergen, May 2007

# Contents

# Introduction

*Warming of the climate system is unequivocal, as is now evident from observations of increases in global average air and sea temperatures* (Solomon et al. 2007). The Intergovernmental Panel on climate change, IPCC, further claims that this observed increase in global average temperatures, with 90% certainty, is due to the observed increase in anthropogenic greenhouse gas concentration. As the greenhouse gas which, in total, causes the most radiative forcing[1], $CO_2$ is considered as the most important.

The global atmospheric concentration of $CO_2$ has increased from pre-industrial value of about 280 ppm (parts per million), to 379 ppm in 2005; todays atmospheric concentration exceeds by far the level of $CO_2$ over the last 650,000 years (Solomon et al. 2007). Measurements from ice cores in Antarctica shows that the level of $CO_2$ concentration has been quite steady at about 275-284 ppm. from around year 1000 and to the industrial period (Etheridge et al. 1998). From the Mauna Loa observatory, at Hawaii, we have continuous records of the atmospheric concentration since 1958. These records shows an average annual increase of 1.4 ppm (Keeling and Whorf 2005).

The main source for the increased atmospheric concentration of $CO_2$ over the last 50 years, results from emissions, due to use of fossil fuel. Most of these emissions come from power plants (coal, gas and oil), refineries, and different types of petrochemical industry. That is, emission from point sources. Thus, we can separate and capture the $CO_2$ from these emission sources.

Aquifers are geological formations in the ground; reservoirs containing water. Overlain by an impermeable caprock, many of these aquifers are suitable for storage of $CO_2$. Such formations are found all over the world. The potential of $CO_2$ storage in geological formations, such as aquifers, are huge. Available evidence suggests that there is a worldwide potential of storing at least 2000 Gt of $CO_2$ in such formations (IPCC 2005). For the purpose of stabilising the atmospheric concentration of $CO_2$, geological storage could contribute with 15-55%, until around 2100.

When injecting $CO_2$ into an under-ground formation, such as an aquifer, we will be inter-

[1]The difference between incoming radiation energy and outgoing radiation energy, in which a positive radiative forcing tends to warm the climate system.

ested in storing the $CO_2$ for thousands of years. When considering millions of tons of $CO_2$, we are looking at a large scale problem, both in time and space. When reservoirs often has irregular structure with variations on the scale of micrometers, numerical simulations will be demanding.

In order to develop a model, which solves for the reservoir flow in a reasonable amount of time, we will have to make some assumptions on the reservoir/aquifer. When we want to solve for the flow on a reservoir scale ($10^3 - 10^5$ meters), we will further neglect some of the effects on the pore scale ($10^{-6}$ meters). By assuming that the phases are separated by a *sharp* interface, Nordbotten and Celia (2006b) manage to carry out a similarity solution for the injection of $CO_2$ into a confined aquifer.

In this thesis, we will look at the stability for the model of Nordbotten and Celia (2006b). In Chapter 1 we give a general presentation of reservoir mechanics. The concepts of dimensional analysis and self-similarity are treated in Chapter 2. Based upon the theory from these two chapters, we can show the derivation of the analytical model of Nordbotten and Celia (2006b) in Chapter 3. Stability is already proved for the case of high injection rates (Nordbotten and Celia 2006b). In order to study the stability for for lower injection rates, we consider linear stability in Chapter 4 and 5. By the linear analysis in Chapter 4 we impose a criterion on the linear stability. By numerical tools, we will further investigate this problem in Chapter 5. Here we will present the results, showing the region of stability for both the linear stability, from Chapter 4, and the non-linear stability analysis of Nordbotten and Celia (2006b). In Chapter 6 we summarise and conclude the thesis.

# Chapter 1

# Reservoir Mechanics

In reservoir mechanics we study the motion of fluids in porous media. A reservoir is a porous geological structure, with fluids, gas or liquid, filling the void space. Some reservoirs are overlain by an impermeable cap rock, which acts as a seal (Hyne 1984). Such formations are of special economical interest, since they may trap buoyant fluids like oil and gas. A further application of these formations lies in the long term storage of greenhouse gases.

In this chapter we will look at some of the general theory of reservoir mechanics. The theory is based upon the book of Pettersen (1990). We will start by considering Darcy's law, and the basic reservoir and fluid parameters describing reservoir flow. Next, we introduce the equation of continuity, which follows from mass conservation. We will consider two-phase flow, and some of the effects due to the interaction between two phases[1]. Two model equations, the saturation equation and the Buckley-Leverett equation, will then be derived.

## 1.1 Darcy's Law

### 1.1.1 Porous Media

Most reservoir rocks and formations are made by compression of minerals. These rocks may be considered as solid, but in reality consist of a fine structure of pores and grains. We will refer to such materials as porous media. The different porous media are characterised by their *porosity* and *permability*. These rock parameters are discussed below.

The porosity, $\phi$, of a material sample is the fraction of its total volume occupied by pores. It is defined as

[1] A phase can be a composition of several components, and sometimes different fluids. In reservoir mechanics we are usually dealing with the three fluids, oil, gas, and water, often referred to as three phases. However, if the pressure is low enough, some oil will evaporate into gas, and we say that we have a composition of gas in the oil phase.

$$\phi = \frac{V_{\text{pores}}}{V_{\text{total}}}\,, \tag{1.1}$$

where $V_{\text{total}}$ is the volume of the entire sample and $V_{\text{pores}}$ is the volume of all the pores in that sample.

In general, we distinguish between two types of porosity, absolute and effective. Equation (1.1) represents the absolute porosity, which is independent upon the connections of the pores. For the effective porosity, $\phi_{\text{eff}}$, we exchange $V_{\text{pores}}$ in (1.1) by the volume of interconnected pores. Since fluids only flow through interconnected pore channels, this parameter provides more information about the amount of fluid able to flow through such a medium. Thus, we will further be using this latter porosity, and for simplicity we denote $\phi_{\text{eff}}$ by $\phi$.

In a reservoir, the geometry of the pores is usually not known. This makes it difficult to use a hydrodynamic formulation for reservoir flow. Instead we use Darcy's Law[2]:

$$\mathbf{u} = -\frac{\mathbf{K}}{\mu}(\nabla \mathbf{p} + \rho g \mathbf{k})\,. \tag{1.2}$$

This is an empirical law, and the permability $\mathbf{K}$ is an empirical parameter. Furthermore, $\mu$ is the viscosity and $\rho$ denotes the density of the fluid, $\mathbf{p}$ represents the pressure, and $g$ is here the gravitational constant. The last term in (1.2) represents the variation of the hydrostatic pressure in the vertical direction, where $\mathbf{k}$ is the vertical unit vector pointing upward.

### 1.1.2 The Parameters of Darcy's Law

Since the diameter of the pores in reservoirs often are on the scale of micro meters ($10^{-6}$m), friction against the porewall will be a dominant factor for describing the flow. The viscosity $\mu$ is a measure for the internal friction of a fluid, and thus inversely proportional to the flow velocity $\mathbf{u}$ (see Equation (1.2)). Furthermore, $\mu$ is a scalar function depending on the pressure.

[2]Henry Darcy was a French engineer, who conducted experiments with vertical water-flow through different types of sand and rock formations, in order test Dutch dikes. He used a large cylindrical iron pipe filled with sand, and measured the flow rate of water from a tap at the bottom, when water was injected from the top. Mercury manometers were used for measuring the pressure, one above and one below the sand column. The measurements was however expressed in terms of the heights of the water column in equivalent water manometers. In 1856 he could present his results, showing that the waterflow was proportional to the pressure difference measured by the water heights, and inversely proportional to the height of the sand column (Hubbert 1956). The proportional constant was dependent upon the type of porous medium used in the experiment. This law has later been tested with different types of fluids, flowing not only vertical, but in various types of angles. It has been slightly modified, but is still known as Darcy's law.

The permability, $\mathbf{K}$, is a parameter that represents the structure and geometry of the pores in a porous medium. It is a rock parameter, and thus independent on which fluids that flows through the porous medium. Generally, $\mathbf{K}$, is a second order tensor defined by Darcy's law.

A reservoir associated with constant permability is denoted as homogeneous. Otherwise, if the permability is spatial dependent, the reservoir is said to be heterogeneous. Furthermore, a permability field which is directional dependent is called anisotropic.

## 1.2 The Equation of Continuity

Consider an arbitrary fixed geometrical volume $\Omega$ inside a reservoir. The principle of mass conservation says that the change of total mass inside this volume, must be balanced by the flux of mass over the boundary, $\sigma$, and a possible source or sink term inside of $\Omega$. Consider that there is only one fluid flowing through the reservoir. The concentration of fluid inside $\Omega$ will then be expressed by $\phi\rho$, where $\phi$ is the porosity and $\rho$ denotes the density of the fluid. When $\mathbf{u}$ represents the velocity of the fluid flow, and $Q$ denotes the source (or sink) term, we get

$$\frac{\partial}{\partial t}\int_{\Omega}(\phi\rho)\,\mathrm{d}\Omega + \int_{\sigma}(\rho\mathbf{u}\cdot\mathbf{n})\,\mathrm{d}\sigma = \int_{\Omega} Q\mathrm{d}\Omega\,. \tag{1.3}$$

In the second term of this equation, $\mathbf{n}$ denotes the normal vector. This vector is defined everywhere on the boundary $\sigma$ as the unit vector, which is perpendicular to the boundary, and points out of $\Omega$. By using Gauss formula, we can further convert the second integral into a volume integral. Also, since the geometric volume $\Omega$ is said to be fixed, it will not be time-dependent. Hence, we can put the time-derivative inside the integration in the first term of (1.3). This implies,

$$\int_{\Omega}\left(\frac{\partial}{\partial t}(\phi\rho) + \nabla\cdot(\rho\mathbf{u})\right)\mathrm{d}\Omega = \int_{\Omega} Q\mathrm{d}\Omega\,.$$

When we know that this relation holds for an arbitrary geometric volume $\Omega$, we further obtain the general equation of continuity,

$$\frac{\partial}{\partial t}(\phi\rho) + \nabla\cdot(\rho\mathbf{u}) = Q\,. \tag{1.4}$$

## 1.3 Two-Phase Flow

Let us now consider two phases flowing in the same porous medium. For simplicity, we shall assume that the phases are immiscible.

### 1.3.1 Model Equations for Two-Phase Flow

The saturation of fluid $i$, is denoted by $S_i$, and defined as the fraction of pore space occupied by fluid $i$. The presence of several fluids, will reduce the pore space, and thus the permability for each of the fluids. In order to correct for this reduction of pore space, we split the permability into one that is only dependent on the structure of the pore space, $\mathbf{K}$, and one that only depends on the saturation of the other fluids, $k_{r,i}(S)$. That is,

$$\mathbf{K}_i(S) = \mathbf{K} \cdot k_{r,i}(S)\,, \quad \text{where} \quad \sum_{i=1}^{i=2} k_{r,i}(S) \leq 1\,.$$

For simplicity we also introduce another parameter, the mobility

$$\lambda_i(S) = \frac{k_{r,i}(S)}{\mu_i}\,.$$

By including these new parameters into Darcy's law (1.2) and the equation of continuity (1.4), we can write the model equations for two-phase flow as follows:

$$\frac{\partial}{\partial t}(\phi \rho_i S_i) + \nabla \cdot (\rho_i \mathbf{u}_i) = Q \quad \text{for} \quad i = 1, 2\,, \tag{1.5}$$

$$\mathbf{u}_i = -\mathbf{K}\lambda_i(\nabla \mathbf{p}_i + \rho_i g \mathbf{k}) \quad \text{for} \quad i = 1, 2\,, \tag{1.6}$$

$$S_1 + S_2 = 1\,. \tag{1.7}$$

### 1.3.2 The Saturation Equation

By combinding the equations, (1.5)-(1.7), we are able to derive the so-called saturation equation. For simplicity, we will look at the case of one dimensional immiscible flow (see Figure 1.1), and the following assumptions are made:

- one dimensional flow
- immiscible and incompressible fluids
- homogeneous reservoir
- constant viscosity
- constant porosity
- no source or sink terms ($Q = 0$)

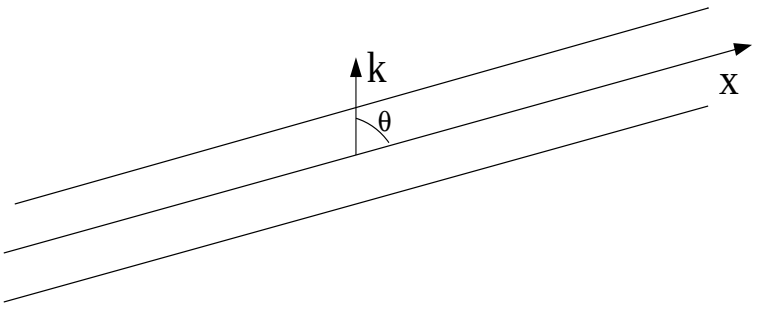


Figure 1.1: Two phase flow in one dimension $x$.

When adding the equation of continuity (1.5) for each of the incompressible fluids together, and use relation (1.7), we get

$$\frac{\partial}{\partial x}(u_1 + u_2) = 0 \, .$$

A flow pattern which satisfies this equation is said to be divergence free. This further leads to the relation,

$$u = u_1 + u_2 \, , \tag{1.8}$$

where $u$ is a constant.

By rearranging (1.6) we can get an equation for the pressure,

$$\frac{\partial p_i}{\partial x} = -\frac{u_i}{k_x \lambda_i} - \rho_i g \cos(\theta) \quad \text{for} \quad i = 1, 2 \, . \tag{1.9}$$

In this equation, $k_x$ is the constant permability in the direction of $\mathbf{x}$, while $\theta$ is the angle between the $\mathbf{x}$-axis and the vertical axis, $\mathbf{k}$, pointing upward (see Figure 1.1). We further subtract the equations in (1.9) from each other, obtaining

$$\frac{\partial}{\partial x} p_{\text{cap}} = \frac{u_1}{k_x \lambda_1} + \rho_1 g \cos(\theta) - \frac{u_2}{k_x \lambda_2} - \rho_2 g \cos(\theta) \, . \tag{1.10}$$

Here we have introduced the capillary pressure, $p_{\text{cap}} = p_2 - p_1$. By relation (1.8), we can express the velocity of the second phase by the velocity of the first phase; $u_2 = u - u_1$. Substituting this expression into (1.10), we get

$$\frac{\partial}{\partial x} p_{\text{cap}} = \frac{u_1}{k_x} \left( \frac{1}{\lambda_1} + \frac{1}{\lambda_2} \right) - \frac{u}{k_x \lambda_2} - (\rho_2 - \rho_1) g \cos(\theta) \, .$$

We can now write the expression for the velocity of phase 1:

$$\begin{aligned} u_1 &= \frac{\lambda_1\lambda_2}{\lambda_1+\lambda_2}\left(k_x\frac{\partial p_{\text{cap}}}{\partial x}+\frac{u}{\lambda_2}+k_x(\rho_2-\rho_1)g\cos(\theta)\right) \\ &= uf(S)+k_x\lambda_2 f(S)\left(\zeta+\frac{\partial p_{\text{cap}}}{\partial x}\right), \end{aligned} \tag{1.11}$$

where

$$f(S)=\frac{\lambda_1}{\lambda_1+\lambda_2} \quad \text{and} \quad \zeta=(\rho_2-\rho_1)g\cos(\theta)\,.$$

In the same way as for the velocity, we can use relation (1.7) and represent the saturation of phase 2 by the saturation of phase 1; $S_2 = 1 - S_1$. Since we are solving for the velocity of phase 1, we choose to let $S$ represent the saturation of this phase. For simplicity we introduce another function,

$$F(S)=f(S)+\lambda_2 f(S)\frac{k_x}{u}\zeta\,.$$

Substituting $F(S)$ into (1.11), we get

$$u_1 = uF(S)+k_x\lambda_2 f(S)\frac{\mathrm{d}}{\mathrm{d}S}p_{\text{cap}}(S)\frac{\partial S}{\partial x}\,.$$

Finally, by substituting this expression into the equation of continuity (1.5) for phase 1, we obtain

$$\frac{\partial S}{\partial t}+\frac{u}{\phi}\frac{\partial F(S)}{\partial x}+k_x\frac{\partial}{\partial x}\left(\lambda_2 f(S)\frac{\mathrm{d}}{\mathrm{d}S}p_{\text{cap}}(S)\frac{\partial S}{\partial x}\right)=0\,, \tag{1.12}$$

which is the saturation equation for two-phase flow in one dimension. The second term in Equation (1.12) is often refered to as the advection term, while the last term often is called the diffusion term, or the capillary term.

### 1.3.3 The Buckley-Leverett Equation

When dealing with high injection rates or large-scale problems (in $x$ and $t$), the advection term is often more dominant than the diffusion term. High injection rates, implies large values of $u$, which is proportional to the magnitude of the advection term. Also, scaling the dimension of $x$ and $t$ by a factor $a > 1$, implies reducing the magnitude of the terms proportional to $\frac{\partial}{\partial x}$ and $\frac{\partial}{\partial t}$ by a factor $a$, and $\frac{\partial^2}{\partial x^2}$ by a factor $a^2$. Thus, in the case of $a \gg 1$, the diffusion term will get small. Considering these cases, the saturation equation is often approximated by the Buckley-Leverett equation,

$$\frac{\partial S}{\partial t}+\frac{u}{\phi}\frac{\partial F(S)}{\partial x}=0\,. \tag{1.13}$$

In this equation we have neglected the effect of capillary forces. Equation (1.13) is a non-linear hyperbolic equation, and may lead to discontinuous solutions or shock waves. To be able to handle shocks we need to rewrite the equation in integral form and compute weak solutions, see Evans (1998).

For the $CO_2$ problem considered in this thesis, see Chapter 3, the length scale will be of order $10^3 - 10^5$ meters, and injection rates are high. Thus, we will neglect the capillary term, and look for a Buckley-Leverett type of model equation.

# Chapter 2

# Similarity

In this chapter we will present the concept of dimensional analysis, similarity and self-similar phenomena. Dimensional analysis provides a method for reducing the number of governing parameters for a given physical problem. If the phenomenon we are investigating has the feature of self-similarity, we can further simplify the problem by a coordinate transformation.

## 2.1 Physical Quantities and their Units

If we want to make a model of a physical phenomenon, we need to know which physical quantities are important for this phenomenon. A physical quantity is measureable and can be measured due to a chosen system of units. A system of units consist of all the fundamental units needed for the description of a phenomenon. For instance, if we want to compute the average velocity of a moving car over a certain period of time, we will have to consider the two quantities of length and time. If we choose the units for length and time to be meters, m, and seconds, s, this will represent one system of units. In some cases it may be more convenient to use larger units, like kilometers (1000 meter) and hours (3600 seconds) instead of meters and seconds. We will then be dealing with another system of units. These two systems is however said to be of the same class of systems of units. All systems of units that differ only in magnitude, but represents the same physical quantities, belong to the same class. Hence, the two systems of units discussed above will both belong to the class of all systems of units corresponding to these units:

$$\begin{aligned} \text{unit of length} &= \text{m/L}\,, \\ \text{unit of time} &= \text{s/T}\,, \end{aligned} \tag{2.1}$$

where $L$ and $T$ are positive numbers which determine the magnitude of the units.

## 2.2 Dimensions

When going from one system of units to another system of units within the same class, the numerical values of the physical quantities will change according to some scaling factors (see (2.1)). The function that determines these scaling factors are called the dimension functions, or dimensions (Barenblatt 1996). If the numerical value of a quantity are identical in all systems of units within the same class, the quantity is denoted dimensionless.

Let us again consider the moving car. If the car has driven a distance, x, in a period of time, t, the average velocity, $\overline{v}$, of the car over that period of time, must be given by

$$\overline{v} = \frac{x}{t} \,. \tag{2.2}$$

Such a mathematical model of a physical problem must be independent of which system of units, within the class of systems of units for this kind of phenomena (moving car), we which to use. Since the sufficient variables for finding the average velocity are the distance, $x$, and time, $t$, the units for these variables must satisfy Equation (2.1). Thus, the unit for the average velocity, $\overline{v}$, will have to satisfy (T/L)$\cdot$ m/s. If we compare the two systems of units discussed above, one where L and T were equal to 1 and the other where we had L=1/1000 and T=1/3600, we find that 1 m/s = 3.6 km/t.

If we change the unit of the spatial variable, $x$, keeping the units of the other two variables fixed, we see that the numerical values of $x$ and $\overline{v}$ will change, while the numerical value of the time, $t$, remains unchanged. Thus, the dimension of the variable $t$ is independent upon the change in the unit of $x$. By only changing the unit of $t$, keeping the other units fixed, we also observe that the dimension of $x$ is independent upon the change in the unit of $t$. Hence, we say that the two variables $x$ and $t$ are independent. The average velocity, $\overline{v}$, is denoted as a dependent variable.

The dimension of any physical quantity are given as a monomial. That is, a dimension can only be represented by one unit and its scaling factor. When $\overline{v}$ is a dependent variable, the dimension of $\overline{v}$ can be expressed as a product of the dimensions of the independent variables. Furthermore, we are able to construct a dimensionless grouping of our variables, by dividing $\overline{v}$ by the product of equal dimension. That is,

$$\Pi = \frac{\overline{v}}{xt^{-1}} = C \,, \tag{2.3}$$

where $C$ is a constant. A change in the units of any of the variables $\overline{v}$, $x$ or $t$ will not effect the numerical value of $\Pi$. Hence, it is dimensionless. $\Pi^p$ will also be a dimensionless grouping, where $p$ can be any non-zero, finite scalar. Rearanging Equation (2.3), we get $\overline{v} = \frac{Cx}{t}$, which is of the same form as Equation (2.2), and is the only physical relationship between these variables.

## 2.3 Dimensional Analysis

Let us now consider a more general case, where we want to determine a relationship,

$$x = f(y_1, y_2, \ldots, y_n) \,, \tag{2.4}$$

from a certain physical phenomenon. Let us further assume that $m$ of the variables, $\mathbf{y}$, has independent dimensions, while the other $k = n - m$ variables have dimensions which can be expressed as products of powers of the independent dimensions of the first $m$ variables. Thus, Buckingham's $\Pi$-theorem says:

**Theorem 2.3.1 (Buchingham's $\Pi$-theorem)** *A physical relationship between some dimensional quantity and several dimensional governing parameters can be rewritten as a relationship between some dimensionless parameter and several dimensionless products of the governing parameters; the number of dimensionless products is equal to the total number of governing parameters minus the number of governing parameters with independent dimensions.*

We will show that Equation (2.4) can be expressed as a relation of $k+1$, rather than $n+1$ parameters.

We denote the $m$ variables with independent dimensions by $a_1, a_2, \ldots, a_m$ and the other $k$ variables by $b_1, b_2, \ldots, b_k$. In order for Equation (2.4) to be valid in all systems of units within the represented class, the dimensions and units on both sides have to be equal. This means that a dimensionless parameter $\Pi$ can be represented by some product of $x$ and the variables $\mathbf{a}$. The dimension of each of the variables $\mathbf{b}$ can also be combined with some product of powers of the dimensions of $\mathbf{a}$, providing another $k$ dimensionless variables. All these can be written as follows:

$$\Pi = \frac{x(a_1, a_2, \ldots, a_m, b_1, b_2, \ldots, b_k)}{a_1^{p_1} \cdot a_2^{p_2} \cdots a_m^{p_m}} \,, \tag{2.5}$$

$$\Pi_i = \frac{b_i}{a_1^{q_{1,i}} \cdot a_2^{q_{2,i}} \cdots a_m^{q_{m,i}}} \,, \quad \text{for} \quad i = 1, 2, \ldots, k \,, \tag{2.6}$$

where the exponents $p_j$ and $q_{j,i}$ are some finite scalars satisfying the equation. You can always use more than one variable $b_i$ in the expression for any of the dimensionless variables $\Pi_i$. The dimensional analysis provides no method of choosing the best dimensional variables, it only states that there exists $k$ independent dimensionless variables. However, by choosing the dimensionless variables as in (2.6), we can represent each variable $b_i$ by

$$b_i = a_1^{q_{1,i}} \cdot a_2^{q_{2,i}} \cdots a_m^{q_{m,i}} \cdot \Pi_i \,, \quad \text{for} \quad i = 1, 2, \ldots, k \,. \tag{2.7}$$

Substituting (2.7) into (2.5), we can then express our dimensionless variable $\Pi$ as,

$$\Pi = F(a_1, a_2, \ldots, a_m, \Pi_1, \Pi_2, \ldots, \Pi_k) \,. \tag{2.8}$$

It can further be shown that it is always possible to transform the system of units to another system, within the same class, such that any of the variables, $a_i$, with independent dimensions can be changed by an arbitrary factor, while the rest of the variables with independent dimensions remains unchanged (Barenblatt 1996). The dimensionless variables are not effected by the change of any of these variables $a_i$. Hence, $\Pi$, from (2.8), will only be a function of the other dimensionless variables, and so we obtain

$$\begin{aligned} x &= f(a_1, a_2, \ldots, a_m, b_1, b_2, \ldots, b_k) \\ &= a_1^{p_1} \cdot a_2^{p_2} \cdot \cdots \cdot a_m^{p_m} \cdot \phi(\Pi_1, \Pi_2, \ldots, \Pi_k) \, . \end{aligned}$$

This shows that Equation (2.4) can be expressed by $k+1$, rather than $n+1$ variables.

## 2.4 Similarity

An engineer may want to test the carrying capacity of a bridge or the load capacity of a boat. Such tests are often both difficult and costly to do in full scale, and in many cases we would want these tests to be done before the bridge or boat is even built. By using the principles of similarity, we can scale the dimensions of the bridge and the boat and construct prototypes of these, in more convenient dimensions. By similarity transformations we may preform tests on these prototypes, which are *similar* to what we would want to test the bridge or boat for.

Two physical phenomena are said to be *similar* if they only differ in respect of numerical values of the dimensional parameters, while the dimensionless parameters are identical (Barenblatt 1996). In geometry, the angles are the dimensionless paremeters. Thus, if we want to transform a triangle into a similar triangle of different magnitude, we must ensure that the angles remain unchanged. Hence, every triangle with identical angles are similar.

Time-dependent phenomena are a bit more complicated to handle. Mathematical modeling of such phenomena often leads to partial differential equations, which can be difficult to solve. A time dependent phenomenon is said to be *self-similar* if the spatial distribution of its properties at different times can be obtained from one another by a similarity transformation (Barenblatt 1996).

Consider the solution, $u(x,t)$, of a partial differential equation. We introduce a coordinate transformation,

$$\chi = \frac{x}{x_0(t)} \, , \tag{2.9}$$

where $x_0(t)$ is a time dependent scale function for $x$. If $u(x,t)$ is self-similar, there will be two scale functions $x_0(t)$ and $v(t)$, so that the solution $u(x,t)$ can be represented by,

$$u(x,t) = v(t)w(\chi) \; .$$

The coordinate transformation, (2.9), is then called a similarity transformation. Choosing $v(t)$ as a scale for the solution $u(x,t)$, we can represent this scaled solution by $w(\chi)$. Thus, we have transformed the time-dependent problem into a steady-state problem, for new (self-similar) coordinates $\frac{u(x,t)}{v(t)}$ and $\chi$. The partial differential equation is then reduced to an ordinary differential equation.

# Chapter 3

# The Model

In this chapter we will present the mathematical model. This is the analytical model of Nordbotten and Celia (2006b), for $CO_2$ injection into deep saline aquifers. Based upon the equations from Chapter 1, we will show the derivation of this model. By neglecting capillary pressure, we will look for an equation of the same form as the Buckley-Leverett equation (see (1.13)). By a similarity transformation, we further transform the model from a partial differential equation to an ordinary differential equation. The stability of the model equation, will be discussed in more detail in the next chapters.

## 3.1 Physical Interpretation

We consider injection of $CO_2$ into a confined aquifer, bounded by an impermeable caprock above and below. To facilitate analytical treatment, we approximate the porosity, permability and thickness of the aquifer as homogeneous. We are interested in injection from a vertical well, and assume the $CO_2$ to spread radially out from this well. We will not consider stability in the angular coordinate, and assume that we have radial symmetry. Furthermore we approximate the flux of $CO_2$ out of the well ($r = 0$) to be constant in the radial direction.

When these aquifers, typically are located around thousand meters below the ground, they will contain saline water. We will, however, in the following refer to this resident fluid as the water phase. For simplicity we neglect all chemical processes at the interface, and assume that the two phases, $CO_2$ and water, are immiscible. An extention for miscible flow has been done by Nordbotten and Celia (2006b). We will also approximate both fluids to be incompressible and the viscosity of both fluids to be constant.

Some of the saline water will not be able to move while $CO_2$ is injected, and remains as residual saturation in the region of the $CO_2$ phase. We will further be referring to the *region of $CO_2$*, as the region consisting of $CO_2$ and residual water. Since the porosity and the permeability are approximated as homogeneous, we assume the residual saturation of

water to be evenly distributed within this region of $CO_2$.

We will not be considering the interface at the pore scale, but assume that there is a transition zone, of finite length, separating the region of $CO_2$ from the region of water (see Figure 3.1). Furthermore, we will assume this zone to be thin compared to the region of $CO_2$, and thus approximate it by a *sharp* interface. That is, we allow for a discontinuity in the pressure and the fluid parameters over the transition zone. We will refer to this zone as the interface.

Based upon these approximations, we will derive an analytical model for the injection process. This fluid flow system will be dominated by density forces and viscous forces. Since $CO_2$ is both less dense and less viscous than water, we expect the $CO_2$ phase to flow on top of the water phase, forming an fluid interface as shown in Figure 3.1. The equation we get, is a nonlinear parabolic equation, with both a transport term and a diffusion term. We will have transport of $CO_2$ in the radial direction, balanced by a diffusion term caused by gravity override. The equation will, however, degenerate to a first order transport equation at the vertical boundaries of the aquifer. Thus, the model looses its parabolic feature, and will support finite propagation speed of disturbances. That is, the end point of the $CO_2$ phase, $r_0$ (see Figure 3.1), will be bounded for $t < \infty$.

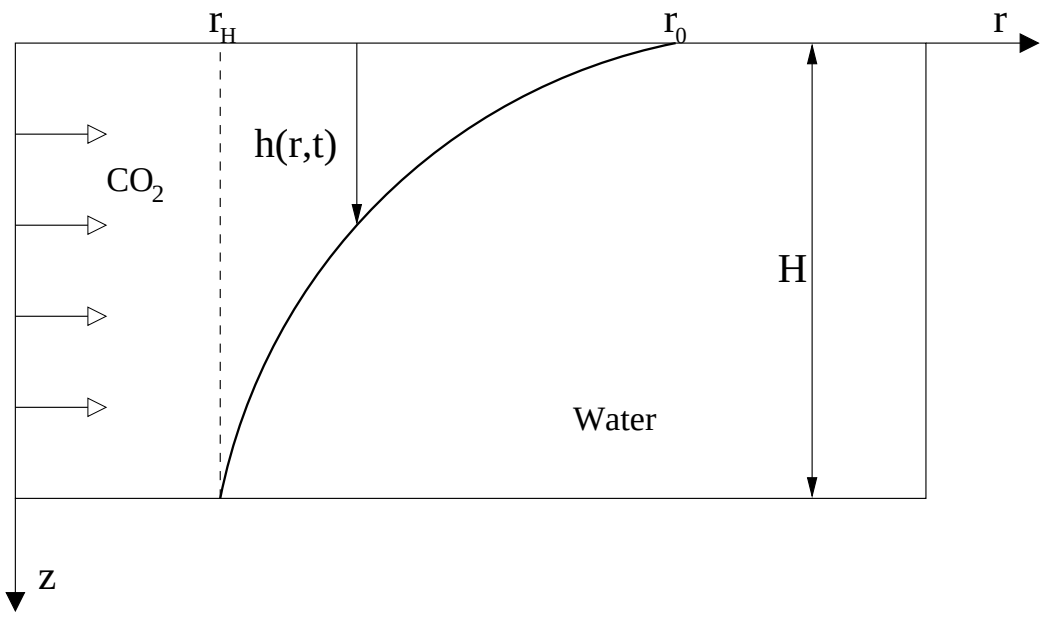


Figure 3.1: The injection process.

## 3.2 Modeling the Interface

Since we have radial symmetry, we only need to consider a two dimensional problem. We then define $h(r,t)$ to be the vertical distance from the top of the aquifer, to the interface (see Figure 3.1). Hence, $h(r,t)$ will be a function for the location of the interface.

Consider now Darcy's law for fluid $i$. From Equation (1.6), we have

$$\mathbf{u}_i = \begin{pmatrix} u_{r,i} \\ u_{z,i} \end{pmatrix} = \begin{pmatrix} -k_r \lambda_i \frac{\partial p_i}{\partial r} \\ -k_z \lambda_i \left[ \frac{\partial p_i}{\partial z} - \rho_i g \right] \end{pmatrix} . \tag{3.1}$$

Rearranging the vertical component of this equation, we get an expression for the derivative of the pressure,

$$\frac{\partial p}{\partial z} = -\frac{u_{z,i}}{k_z \lambda_i} + \rho_i g \, .$$

We want to derive a relation for the pressure in the aquifer, and thus integrate the equation from $z = H$ to $z = 0$, obtaining

$$\begin{aligned} \int_{z=H}^{z=0} \frac{\partial p}{\partial z} \mathrm{d}z &= -\int_{z=H}^{z=h(r,t)} \left( \frac{u_{z,w}}{k_z \lambda_w} - \rho_w g \right) \mathrm{d}z \\ &\quad - p_{\mathrm{cap}} - \int_{z=h(r,t)}^{z=0} \left( \frac{u_{z,c}}{k_z \lambda_c} - \rho_c g \right) \mathrm{d}z \, . \end{aligned} \tag{3.2}$$

On the right-hand side, we have split the integral into one for the region of $CO_2$ and one for the region of water (see Figure 3.1), where the subscripts $c$ and $w$ denotes these regions, $CO_2$ and water, respectively. Also, since the pressure is allowed to be discontinuous over the interface, we get a capillary term, $p_{\mathrm{cap}}(r,t) = p(r,t,h_w) - p(r,t,h_c)$; where $h_i$ is the point on the interface closest to the region of phase $i$. When representing the average flux in the vertical direction, by $q_z(r,t)$, Equation (3.2) further implies

$$\begin{aligned} p(r,t,0) - p(r,t,H) \; = \\ - p_{\mathrm{cap}}(r,t) + \frac{q_{z,c}(r,t)}{k_z \lambda_c} + \frac{q_{z,w}(r,t)}{k_z \lambda_w} - \rho_c g h(r,t) - \rho_w g (H - h(r,t)) \, . \end{aligned}$$

Since the horizontal dimension is much greater than the vertical, we assume the flux in the vertical direction to be small relative to the flux in the horizontal direction. Thus, we neglect the terms proportional to $q_z$, and get

$$p(r,t,0) \; = \; p(r,t,H) - p_{\mathrm{cap}}(r,t) - \rho_c g h(r,t) - \rho_w g (H - h(r,t)) \, . \tag{3.3}$$

Furthermore we have considered the $CO_2$ phase above and the water phase below the interface. Thus, we represent the pressure within each of these phases by, $p_c = p(r,t,0)$

and $p_w = p(r, t, H)$, respectively. We choose the pressure in the water phase as our primary variable for the pressure; $p_w = p$. Hence, we can use relation (3.3) and get an expression for the pressure in the $CO_2$ phase,

$$p_c = p - p_{\text{cap}} - \rho_w g H + \Delta\rho g h(r,t), \quad \text{where} \quad \Delta\rho = \rho_w - \rho_c \,.$$

By differentiate this expression with respect to $r$, we also obtain an expression for the derivative of the pressure within the $CO_2$ phase,

$$\frac{\partial p_c}{\partial r} = \frac{\partial p}{\partial r} - \frac{\partial p_{\text{cap}}}{\partial r} + \Delta\rho g \frac{\partial h(r,t)}{\partial r} \,.$$

This relation is of the same form as Equation (1.11). When considering large scales in $x$ and $t$, the dynamic pressure will be the dominant driving force for the radial flux of $CO_2$. Thus, we neglect the capillary term. By substituting for the pressure in Darcy's law (3.1), we then get

$$u_{r,c} = -k\lambda_c \left( \frac{\partial p}{\partial r} + \Delta\rho g \frac{\partial h(r,t)}{\partial r} \right) , \tag{3.4a}$$

$$u_{r,w} = -k\lambda_w \frac{\partial p}{\partial r} \,. \tag{3.4b}$$

Since we have neglected the flux in the vertical direction, we have chosen to denote the homogeneous permability in the radial direction, $k_r$, by $k$, in the following.

Both phases must also satisfy the equation of continuity. By considering $r > 0$, we neglect the source term ($Q = 0$). We integrate (1.5) in the vertical direction, obtaining one equation for the region of $CO_2$ and one for the region of water. That is,

$$\frac{1}{r}\frac{\partial}{\partial r}(r\rho_c u_{r,c} h(r,t)) + \phi(1 - S_{\text{res}})\frac{\partial}{\partial t}(\rho_c h(r,t)) = 0 \,, \tag{3.5a}$$

$$\frac{1}{r}\frac{\partial}{\partial r}(r\rho_w u_{r,w}(H - h(r,t))) + \phi(1 - S_{\text{res}})\frac{\partial}{\partial t}(\rho_w (H - h(r,t))) = 0 \,, \tag{3.5b}$$

where we have used the divergence operator in cylindrical coordinates. The velocity $u_{r,i}$ is given by (3.4a) and (3.4b). Substituting for the velocity, we rewrite (3.5a) and (3.5b) as

$$\frac{\partial h(r,t)}{\partial t} = \frac{1}{\phi(1 - S_{\text{res}})}\frac{1}{r}\frac{\partial}{\partial r}\left( k\lambda_c r h(r,t) \left[ \frac{\partial p}{\partial r} + \Delta\rho g \frac{\partial h(r,t)}{\partial r} \right] \right) , \tag{3.6a}$$

$$\frac{\partial (H - h(r,t))}{\partial t} = \frac{1}{\phi(1 - S_{\text{res}})}\frac{1}{r}\frac{\partial}{\partial r}\left( k\lambda_w r (H - h(r,t)) \frac{\partial p}{\partial r} \right) . \tag{3.6b}$$

Here, we have also used the approximation of incompressible fluids. By combinding these two equation, we can calculate for the pressure. Thus, we add Equation (3.6a) and (3.6b) together;

$$0 = \frac{k}{\phi(1-S_{\text{res}})}\frac{1}{r}\left[\frac{\partial}{\partial r}\left(\lambda_c r h(r,t)\frac{\partial}{\partial r}\left(p+\Delta\rho g h(r,t)\right)\right)\right.$$
$$\left. + \frac{\partial}{\partial r}\left(\lambda_w r(H-h(r,t))\frac{\partial p}{\partial r}\right)\right].$$

The term $k_r/\phi(1-S_{\text{res}})r$ is nonzero for $r>0$, which implies

$$\frac{\partial}{\partial r}\left[\lambda_c r h(r,t)\frac{\partial}{\partial r}\left(p+\Delta\rho g h(r,t)\right)+\lambda_w r(H-h(r,t))\frac{\partial p}{\partial r}\right]=0\,.$$

This equation, we can integrate with respect to $r$:

$$\lambda_c r h(r,t)\frac{\partial}{\partial r}(p+\Delta\rho g h(r,t))+\lambda_w r(H-h(r,t))\frac{\partial p}{\partial r}=C\,. \tag{3.7}$$

From the principle of mass-conservation and the condition that $CO_2$ is injected at a constant rate of flux, $Q_{\text{well}}$, we can determine $C$. The equation of continuity, (1.3), is valid for an arbitrary geometric volume $\Omega$. For a fixed time $t$, we let $\Omega$ represent a cylinder of radius $r$. By evaluating (3.7) at $r>r_0$, where we have $h(r>r_0,t)=0$ (see Figure 3.1), we obtain

$$C=-\frac{Q_{\text{well}}}{2\pi k},\quad \text{where}\quad Q_{\text{well}}=-2\pi r H k\lambda_w\frac{\partial p}{\partial r}\,.$$

Here we have used the Darcy velocity in the radial direction, in the expression for $Q_{\text{well}}$. Substituting for $C$ back into (3.7), we get

$$\frac{\partial p}{\partial r}=-\left[\lambda_c h(r,t)+\lambda_w(H-h(r,t))\right]^{-1}\left[\lambda_c\Delta\rho g h(r,t)\frac{\partial h(r,t)}{\partial r}+\frac{Q_{\text{well}}}{2\pi r k}\right]\,.$$

Finally, by putting this expression into (3.6b) we obtain the model equation for the interface location $h(r,t)$. That is,

$$\frac{\partial h(r,t)}{\partial t}=\frac{\Delta\rho g k\lambda_w}{\phi(1-S_{\text{res}})r}\frac{\partial}{\partial r}\left[\frac{\lambda_c r h(r,t)(H-h(r,t))}{\lambda_c h(r,t)+\lambda_w(H-h(r,t))}\frac{\partial h(r,t)}{\partial r}\right.$$
$$\left.+\frac{Q_{\text{well}}(H-h(r,t))}{2\pi\Delta\rho g k[\lambda_c h(r,t)+\lambda_w(H-h(r,t))]}\right]. \tag{3.8}$$

## 3.3 Dimensionless Form

In order to simplify our mathematical model (3.8), we will transform it into dimensionless form and reduce the number of parameters in the equation. Thus, we need to construct new dimensionless parameters. Equation (3.8) is a relation for the interface location $h(r,t)$, and has a total of 10 parameters: $h$, $r$, $t$, $\phi$, $\Delta\rho$, $k$, $\lambda_c$, $\lambda_w$, $g$ and $Q_{\text{well}}$, where $h$, $r$, $t$ and $\Delta\rho$

have independent dimensions. Buckingham's Π-theorem (2.3.1) then tells us that we can rewrite the equation as a relationship of some dimensionless parameter (representing $h$) and 6 dimensionless products of the governing parameters. That is, we can at least reduce the number of parameters from 10 to 6. However, dependent on the equation, it might be possible to reduce the number of parameters by more than 3. For the transformation of Equation (3.8), we have chosen the following dimensionless parameters:

$$h' \equiv \frac{h}{H}\,, \quad \Gamma \equiv \frac{2\pi\Delta\rho g k \lambda_w H^2}{Q_{\text{well}}}\,, \quad \lambda \equiv \frac{\lambda_c}{\lambda_w}\,,$$
$$\tau \equiv \frac{Q_{\text{well}} t}{2\pi H \phi k (1 - S_{\text{res}})}\,, \quad \eta \equiv \frac{r}{\sqrt{k}}\,. \tag{3.9}$$

It turns out that we only need 5 dimensionless parameters. This is an consequence of the form of the equation alone; the dimensional analysis only guarantees for a reduction of 3 parameters. The choice of these dimensionless parameters seems to be somewhat arbitrary. As noted before, there are no methods for proving that one choice of dimensionless products are better than another. However, it is important that the chosen dimensionless parameters represent the physics of the problem. The interface location $h$, which we want to solve for, is now being represented by the dimensionless parameter $h'$. But $h'$ is only the normalised interface, taking values between 0 and 1, and will thus represent the same physics as $h$. Furthermore, $\Gamma$ will represent the relative importance of density forces ($\Delta\rho$) to viscous forces ($Q_{\text{well}}/\lambda_w$). In our case $\Delta\rho = \rho_w - \rho_c > 0$, which means that we will have $\Gamma > 0$. The other dimensionless parameters are also chosen to represent some physical quantities: $\lambda$ is simply the mobility ratio, $\tau$ represents the time $t$ and $\eta$ is a scaled parameter for the spatial variable $r$. These parameters will also be non-negative. By substituting the dimensionless parameters into Equation (3.8), we obtain an equation for $h'(\eta, \tau)$:

$$\frac{\partial h'}{\partial \tau} = \frac{1}{\eta}\frac{\partial}{\partial \eta}\left[\frac{\Gamma\lambda h'(1-h')\eta}{\lambda h' + (1-h')}\frac{\partial h'}{\partial \eta} + \frac{1-h'}{\lambda h' + (1-h')}\right]\,. \tag{3.10}$$

## 3.4 Self-Similar Transformation

When $CO_2$ is injected into a homogeneous reservoir with radial symmetry, we expect the $CO_2$ to spread equally out in all directions normal to the well at each depth. Thus, the volume of $CO_2$ at time $t$, will be proportional to $Hr(t)^2$. Since we also assume constant injection rate $Q_{\text{well}}$ and incompressible flow, the volume of $CO_2$ divided by the time $t$ must be of constant value at all times. Thus, $t$ will be proportional to $r^2$. In dimensionless variables (see (3.9)), this implies $\tau$ being proportional to $\eta^2$.

The solution $h'(\eta, \tau)$ of Equation (3.10) represents the interface between the region of water and $CO_2$. The shape of this interface will in time change due to gravity forces. We hypothesise that this injection process has the feature of self-similarity, and that Equation (3.10) can be transformed to an ordinary differential equation by the transformation,

$$\chi = \eta^2/\tau \,. \tag{3.11}$$

Transforming the derivatives in Equation (3.10) by this transformation, we get

$$\begin{aligned}
\frac{\partial h'(\eta,\tau)}{\partial \eta} &= \frac{\partial h'(\chi,\tau)}{\partial \chi}\frac{\partial \chi}{\partial \eta} = 2\frac{\eta}{\tau}\frac{\partial h'(\chi,\tau)}{\partial \chi}\,, \\
\frac{\partial h'(\eta,\tau)}{\partial \tau} &= \frac{\partial h'(\chi,\tau)}{\partial \chi}\frac{\partial \chi}{\partial \tau} + \frac{\partial h'(\chi,\tau)}{\partial \tau} = -\frac{\chi}{\tau}\frac{\partial h'(\chi,\tau)}{\partial \chi} + \frac{\partial h'(\chi,\tau)}{\partial \tau}\,.
\end{aligned}$$

Substituting these into (3.10), we obtain

$$-\chi\frac{\partial h'}{\partial \chi} + \tau\frac{\partial h'}{\partial \tau} = 2\frac{\partial}{\partial \chi}\left[\frac{1-h'}{1+(\lambda-1)h'}\left(1 + 2\Gamma\lambda\chi h'\frac{\partial h'}{\partial \chi}\right)\right]\,, \tag{3.12}$$

where $h' = h'(\chi,\tau)$. The differentiation on the right-hand side of Equation (3.12) can be carried out to yield,

$$\begin{aligned}
\tau\frac{\partial h'}{\partial \tau} - \chi\frac{\partial h'}{\partial \chi} = 2\Bigg[&\frac{-[1+(\lambda-1)h' + (1-h')(\lambda-1)]\frac{\partial h'}{\partial \chi}}{[1+(\lambda-1)h']^2}\left(1 + 2\Gamma\lambda\chi h'\frac{\partial h'}{\partial \chi}\right) \\
&+\frac{2\Gamma\lambda(1-h')}{1+(\lambda-1)h'}\left(h'\frac{\partial h'}{\partial \chi} + \chi\left(\frac{\partial h'}{\partial \chi}\right)^2 + \chi h'\frac{\partial^2 h'}{\partial \chi^2}\right)\Bigg]\,,
\end{aligned}$$

and rearranged as,

$$\begin{aligned}
\tau\frac{\partial h'}{\partial \tau}\left(\frac{\partial h'}{\partial \chi}\right)^{-1} = \chi &- \frac{2\lambda}{[1+(\lambda-1)h']^2}\left(1 + 2\Gamma\lambda\chi h'\frac{\partial h'}{\partial \chi}\right) \\
&+4\Gamma\lambda\frac{1-h'}{1+(\lambda-1)h'}\left[h' + \chi\frac{\partial h'}{\partial \chi} + \chi h'\frac{\partial^2 h'}{\partial \chi^2}\left(\frac{\partial h'}{\partial \chi}\right)^{-1}\right]\,.
\end{aligned} \tag{3.13}$$

Here we have assumed that $\frac{\partial h'}{\partial \chi} \neq 0$. If (3.11) represents a similarity transformation, the solution $h'(\chi,\tau)$ will approach the asymptote of $h'(\chi)$. Thus, $h'(\chi,\tau)$ can be represented by $h'(\chi)$ for late times $\tau$, and we need only to solve the following stationary equation:

$$\begin{aligned}
0 = \chi &- \frac{2\lambda}{[1+(\lambda-1)h']^2}\left(1 + 2\Gamma\lambda\chi h'\frac{\mathrm{d}h'}{\mathrm{d}\chi}\right) \\
&+ 4\Gamma\lambda\frac{1-h'}{1+(\lambda-1)h'}\left[h' + \chi\frac{\mathrm{d}h'}{\mathrm{d}\chi} + \chi h'\frac{\mathrm{d}^2 h'}{\mathrm{d}\chi^2}\left(\frac{\mathrm{d}h'}{\mathrm{d}\chi}\right)^{-1}\right]\,.
\end{aligned} \tag{3.14}$$

The stationary solution $h'(\chi)$ is proved to be stable for small values of $\Gamma$ (Nordbotten and Celia 2006b). That is,

$$h'(\chi,\tau) \longrightarrow h'(\chi) \quad \text{as} \quad \tau \to \infty\,, \quad \text{for} \quad \Gamma < \Gamma_c(\lambda). \tag{3.15}$$

Thus, $h'(\chi)$ will be stable with respect to perturbations. The stability proof of Nordbotten and Celia (2006b) is reproduced in Appendix B. There is however no discussion about the magnitude of $\Gamma_c(\lambda)$; Nordbotten and Celia (2006b) only states that there exists such a positive value of $\Gamma$. Typical values of $\Gamma$, will be of order $10^{-2}-10^{2}$ (Bachu, Nordbotten, and Celia 2004), dependent on both the aquifer ($k$ and $H$), the injection rate ($Q_{\text{well}}$) and the fluid parameters ($\rho$ and $\lambda$). The fluid parameters will further depend on the temperature and depth of the aquifer. The mobility ratio, $\lambda$, between $CO_2$ and water, will typically be $5-25$ (Nordbotten and Celia 2006a).

We will investigate the value of $\Gamma_c$, for different values of $\lambda$ in Chapter 5. This analysis shows that $\Gamma_c(\lambda)$ will be of order $10^{-1}$, for values of $\lambda > 5$. In order to study the stability for other values of $\Gamma$, we will focus on linear stability in the next chapter.

# Chapter 4

# Analysis

In this chapter we will study the linear stability of the time-dependent equation, given by Equation (3.13). When considering a linearised solution of this equation, we impose a criterion for the stability. This criterion will depend upon the solution of the stationary equation (3.14). Thus, we first look at the properties of this equation.

## 4.1 Properties of the Stationary Equation

With a slight abuse of notation, we write the stationary equation (3.14) as

$$\begin{aligned} 0 &= \chi - \frac{2\lambda}{[1+(\lambda-1)h_0]^2}\left(1 + 2\Gamma\lambda\chi h_0 \frac{\mathrm{d}h_0}{\mathrm{d}\chi}\right) \\ &\quad + 4\Gamma\lambda \frac{1-h_0}{1+(\lambda-1)h_0}\left[h_0 + \chi\frac{\mathrm{d}h_0}{\mathrm{d}\chi} + \chi h_0 \frac{\mathrm{d}^2 h_0}{\mathrm{d}\chi^2}\left(\frac{\mathrm{d}h_0}{\mathrm{d}\chi}\right)^{-1}\right], \end{aligned} \tag{4.1}$$

Here, $h_0 = h_0(\chi)$ is the steady-state solution, where $\chi$ is the self-similar variable given by (3.11). The equation will further be valid in the interval $\chi \in \langle \chi_1, \chi_0 \rangle$, where the boundary points are defined as:

$$\chi_0 = \{\chi : h_0(\chi) = 0\}, \tag{4.2}$$

$$\chi_1 = \{\chi : h_0(\chi) = 1\}. \tag{4.3}$$

Thus, we have a boundary-value problem. Since all the terms in (4.1) are non-zero and bounded in the interval $\chi \in \langle \chi_1, \chi_0 \rangle$, the solution $h_0(\chi)$ will be continuous within this interval. Furthermore, the equation degenerates at the boundaries $\chi_0$ and $\chi_1$, where $h_0(\chi_0) = 0$ and $h_0(\chi_1) = 1$. Since we have assumed no leakage of $CO_2$, we consider $h_0(\chi) \in [0, 1]$ and define $h_0(\chi) = 1$ for $\chi \leq \chi_1$, and $h_0(\chi) = 0$ for $\chi \geq \chi_0$ (see Figure 4.1).

Since Equation (4.1) degenerates at the boundary points, $h_0(\chi)$ may not be smooth at

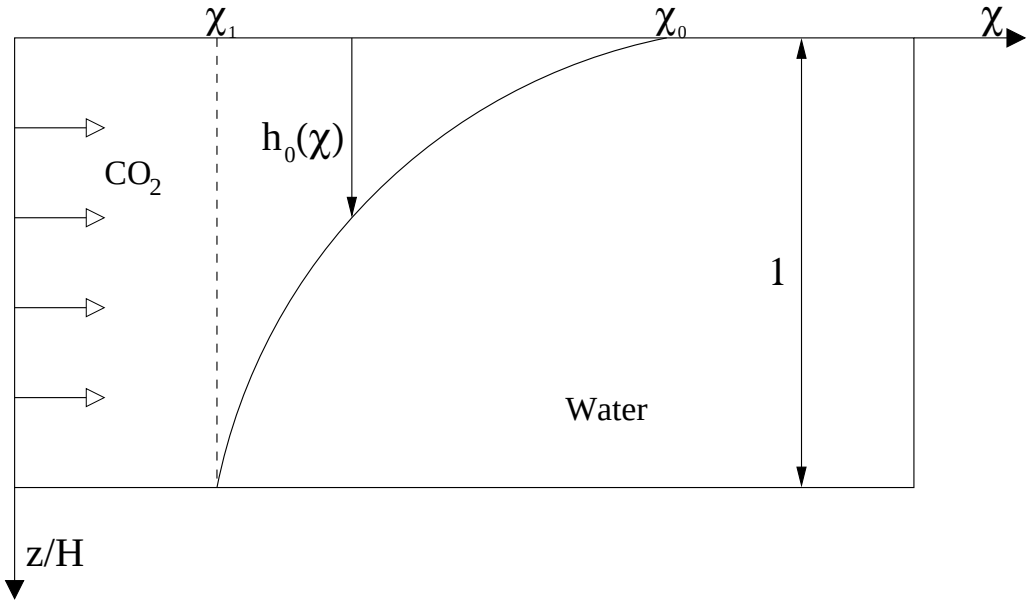


Figure 4.1: The interface location, $h_0(\chi)$, between the region of $CO_2$ and water, in self-similar coordinates

these points. Hence, the derivative of $h_0(\chi)$ is not in general defined at the boundaries. However, by considering the limit from one side only, we can get an expression for the derivative at $\chi_0^-$ and $\chi_1^+$. By substituting (4.2) and (4.3) into (4.1), Equation (4.1) degenerates to a couple of first order equations. These are,

$$\begin{aligned} 0 &= \chi_0 - 2\lambda + 4\Gamma\lambda\chi_0 \frac{\mathrm{d}h_0}{\mathrm{d}\chi}\bigg|_{\chi=\chi_0^-}, \\ 0 &= \chi_1 - \frac{2}{\lambda} - 4\Gamma\chi_1 \frac{\mathrm{d}h_0}{\mathrm{d}\chi}\bigg|_{\chi=\chi_1^+}. \end{aligned}$$

Hence, the derivative of $h_0(\chi)$ at the boundaries can be written as:

$$\frac{\mathrm{d}h_0}{\mathrm{d}\chi}\bigg|_{\chi=\chi_0^-} = \frac{2\lambda - \chi_0}{4\Gamma\lambda\chi_0}, \tag{4.4a}$$

$$\frac{\mathrm{d}h_0}{\mathrm{d}\chi}\bigg|_{\chi=\chi_1^+} = \frac{\lambda\chi_1 - 2}{4\Gamma\lambda\chi_1}. \tag{4.4b}$$

We now have two conditions for our boundary-value problem. Hence, we can find a unique solution for Equation (4.1) in the interval $\chi \in \langle\chi_1, \chi_0\rangle$. If one of the boundary points ($\chi_0$ or $\chi_1$) is known, it will be sufficient only to know the derivative at this boundary point; the equation can then be solved uniquely. However, when the values of $\chi_0$ and $\chi_1$ are

unknown, both conditions (4.4a) and (4.4b) are necessary.

By differentiating Equation (4.1), we are also able to find expressions for the second derivative of $h_0(\chi)$ at the boundary points (see Appendix A for more details). From (A.2) and (A.3) we get

$$\begin{aligned}\left.\frac{\mathrm{d}^2h_0}{\mathrm{d}\chi^2}\right|_{\chi_0^-} &= \lambda\left(\left.\frac{\mathrm{d}h_0}{\mathrm{d}\chi}\right|_{\chi_0^-}\right)^2 - \frac{2\Gamma+\lambda-1}{2\Gamma\chi_0}\left.\frac{\mathrm{d}h_0}{\mathrm{d}\chi}\right|_{\chi_0^-} - \frac{1}{8\Gamma\lambda\chi_0} \\ &= \frac{\chi_0^2 - 2\chi_0 + 2\Gamma\chi_0 - 2\lambda\chi_0 - 8\Gamma\lambda + 4\lambda}{16\Gamma^2\lambda\chi_0^2}\,, \qquad (4.5a)\\ \left.\frac{\mathrm{d}^2h_0}{\mathrm{d}\chi^2}\right|_{\chi_1^+} &= -\frac{1}{\lambda}\left(\left.\frac{\mathrm{d}h_0}{\mathrm{d}\chi}\right|_{\chi_1^+}\right)^2 - \left(\frac{1}{\chi_1} - \frac{\lambda-1}{2\Gamma\lambda^2\chi_1}\right)\left.\frac{\mathrm{d}h_0}{\mathrm{d}\chi}\right|_{\chi_1^+} + \frac{1}{8\Gamma\chi_1} \\ &= \frac{8\Gamma\lambda^2 - 2\Gamma\lambda^3\chi_1 - \lambda^2\chi_1^2 + 2\lambda^2\chi_1 + 2\lambda\chi_1 - 4\lambda}{16\Gamma^2\lambda^3\chi_1^2}\,. \qquad (4.5b)\end{aligned}$$

### 4.1.1 Conservation of $CO_2$

The boundary conditions (4.4a) and (4.4b) further lead to a condition on the volume of $CO_2$. By assuming $\frac{\partial h'}{\partial \tau} = 0$ in Equation (3.12), this equation becomes equivalent to Equation (4.1). That is,

$$-\chi\frac{\mathrm{d}h_0}{\mathrm{d}\chi} = 2\frac{\mathrm{d}}{\mathrm{d}\chi}\left[\frac{1-h_0}{1+(\lambda-1)h_0}\left(1+2\Gamma\lambda\chi h_0\frac{\mathrm{d}h_0}{\mathrm{d}\chi}\right)\right]\,. \qquad (4.6)$$

By integrating this equation from $\chi = 0$ to $\chi = \chi_0$, we get

$$\begin{aligned}-\int_0^{\chi_0}\chi\frac{\mathrm{d}h_0}{\mathrm{d}\chi}\mathrm{d}\chi &= 2\left[\frac{1-h_0}{1+(\lambda-1)h_0}\left(1+2\Gamma\lambda\chi h_0\frac{\mathrm{d}h_0}{\mathrm{d}\chi}\right)\right]\Bigg|_{\chi=0}^{\chi=\chi_1} \\ &\quad + 2\left[\frac{1-h_0}{1+(\lambda-1)h_0}\left(1+2\Gamma\lambda\chi h_0\frac{\mathrm{d}h_0}{\mathrm{d}\chi}\right)\right]\Bigg|_{\chi=\chi_1}^{\chi=\chi_0}\,.\end{aligned}$$

Since the derivative is discontinuous in $\chi_1$, we have split the integration on the right-hand side into to domains. When $h'(\chi) = 1$ for $\chi \in \langle 0, \chi_1]$, the first term on the right-hand side is zero. Using integration by parts on the left-hand side of the equation, we further obtain

$$\begin{aligned}-\chi_0 h_0(\chi_0) + \int_0^{\chi_0} h_0(\chi)\mathrm{d}\chi = 2\Bigg[&\frac{1-h_0(\chi_0)}{1+(\lambda-1)h_0(\chi_0)}\left(1+2\Gamma\lambda\chi_0 h_0(\chi_0)\left.\frac{\mathrm{d}h_0}{\mathrm{d}\chi}\right|_{\chi_0}\right) \\ &- \frac{1-h_0(\chi_1)}{1+(\lambda-1)h_0(\chi_1)}\left(1+2\Gamma\lambda\chi_1 h_0(\chi_1)\left.\frac{\mathrm{d}h_0}{\mathrm{d}\chi}\right|_{\chi_1}\right)\Bigg]\,. \qquad (4.7)\end{aligned}$$

We consider $\frac{\mathrm{d}h_0}{\mathrm{d}\chi}$ to be bounded for $\chi \in \langle \chi_1, \chi_0 \rangle$. This will be proved for $0 < \Gamma < \infty$ and $1 < \lambda < \infty$ in Section 4.1.2. By substituting (4.2) and (4.3) into Equation (4.7), we obtain a dimensionless expression for the volume of $CO_2$ inside the aquifer. That is,

$$\int_0^{\chi_0} h_0(\chi)\mathrm{d}\chi = 2\,. \tag{4.8}$$

This is not an additional condition for the boundary-value problem, but a consequence of the two boundary conditions (4.4a) and (4.4b). However, since we do not know the values of $\chi_0$ and $\chi_1$, the value of the derivatives at these points are unknown as well. By replacing condition (4.4b) with (4.8), we still have two condition for our boundary value problem, in which will give us a unique solution. This will simplify the numerical implementation, presented in the next chapter. The dimensionless formulation (4.8) is further equivalent with the conservation of $CO_2$,

$$\int_0^{r_0} \phi(1 - S_{\mathrm{res}})2\pi r h(r,t)\mathrm{d}r = Q_{\mathrm{well}}t\,,$$

where $r_0$ is the point on $r$ which corresponds to the dimensionless point $\chi_0$ (see Figure 3.1 and 4.1).

Furthermore, we can find a relation for the derivative of $h_0(\chi)$, by integrating (3.12) from 0 to an arbitrary $\chi$. That is,

$$-\chi h_0 + \int_0^{\chi} h_0 \mathrm{d}\chi = 2\left[\frac{1-h_0}{1+(\lambda-1)h_0}\left(1 + 2\Gamma\lambda\chi h_0 \frac{\mathrm{d}h_0}{\mathrm{d}\chi}\right)\right]\,.$$

By rearranging this equation, we get

$$1 + 2\Gamma\lambda\chi h_0 \frac{\mathrm{d}h_0}{\mathrm{d}\chi} = \frac{1+(\lambda-1)h_0}{2(1-h_0)}\left[\int_0^{\chi} h_0 \mathrm{d}\chi - \chi h_0\right]\,. \tag{4.9}$$

Since $h_0(\chi) \in [0,1]$, the integral in (4.9) will be smaller or equal to the value of $\chi$. Also, when $\frac{\mathrm{d}h_0}{\mathrm{d}\chi} \leq 0$, the integral will be greater or equal to the value of $\chi h_0$ (see Figure 4.1). Using these inequalities in (4.9), we get the following inequality:

$$0 \leq 1 + 2\Gamma\lambda\chi h_0 \frac{\mathrm{d}h_0}{\mathrm{d}\chi} \leq \frac{\chi}{2}[1 + (\lambda-1)h_0]\,.$$

### 4.1.2 The Slope of the Stationary Equation

For the derivation of Equation (3.13) and (3.14), from the previous chapter, we considered the interface to be shaped by gravity override (see Figure 4.1), and assumed $\frac{\partial h'}{\partial \chi} < 0$ for $\chi_1 < \chi < \chi_0$. The following Theorem shows that this assumption holds for Equation (4.6).

**Theorem 4.1.1** *Let $0 < \Gamma < \infty$ and $1 < \lambda < \infty$. When $h_0(\chi) \in C^1[\chi_1, \chi_0]$ is the solution of (4.6), with boundary points defined by (4.2) and (4.3) (positive and finite), the derivative of $h_0(\chi)$ will be negative and bounded for all $\chi \in \langle \chi_1, \chi_0 \rangle$.*

*proof.* Consider Equation (4.6). By differentiating the right-hand side of Equation (4.6), we obtain

$$4\Gamma\lambda\left(\frac{\chi h_0(1-h_0)}{1+(\lambda-1)h_0}\right)\frac{\mathrm{d}^2h_0}{\mathrm{d}\chi^2}+\psi(\chi)\frac{\mathrm{d}h_0}{\mathrm{d}\chi}=0\,, \tag{4.10}$$

where

$$\psi(\chi)=\chi-\frac{2\lambda\left(1+2\Gamma\lambda\chi\ h_0\frac{\mathrm{d}h_0}{\mathrm{d}\chi}\right)}{[1+(\lambda-1)h_0]^2}+4\Gamma\lambda\frac{1-h_0}{1+(\lambda-1)h_0}\left(h_0+\chi\frac{\mathrm{d}h_0}{\mathrm{d}\chi}\right)\,.$$

Assume that there is a point $\chi\in\langle\chi_1,\chi_0\rangle$ where $\frac{\mathrm{d}h_0}{\mathrm{d}\chi}=0$. Then,

$$|\psi(\chi)|=\left|\chi-\frac{2\lambda}{[1+(\lambda-1)h_0]^2}+4\Gamma\lambda\frac{h_0(1-h_0)}{1+(\lambda-1)h_0}\right|<\infty\,,$$

and from (4.10) we get

$$4\Gamma\lambda\left(\frac{\chi h_0(1-h_0)}{1+(\lambda-1)h_0}\right)\frac{\mathrm{d}^2h_0}{\mathrm{d}\chi^2}=0\,. \tag{4.11}$$

This can only be satisfied if $\chi=\chi_0$, $\chi=\chi_1$ or $\frac{\mathrm{d}^2h_0}{\mathrm{d}\chi^2}=0$. When considering $\chi\in\langle\chi_0,\chi_1\rangle$, Equation (4.11) implies $\frac{\mathrm{d}^2h_0}{\mathrm{d}\chi^2}=0$. Thus, $h_0(\chi)=C=$ constant. In order to fulfil (4.2) and (4.3), $h_0(\chi)$ will be discontinuous at one of the boundary points, and we have a contradiction. Hence, $\frac{\mathrm{d}h_0}{\mathrm{d}\chi}\neq0$ for all $\chi\in\langle\chi_0,\chi_1\rangle$.

Since $\frac{\mathrm{d}h_0}{\mathrm{d}\chi}\neq0$ and $h_0(\chi)\in C^1[\chi_1,\chi_0]$, $h_0(\chi)$ must be strictly decreasing or increasing within this interval.

When the interface location $h_0(\chi)$ is defined as the distance from the top of the aquifer, through the $CO_2$ phase, and down to the interface (see Figure 4.1), we have $\chi_0>\chi_1$. Otherwise the aquifer is initially fully saturated with $CO_2$. From (4.2) and (4.3) we have $h_0(\chi_0)<h_0(\chi_1)$, which means that $h_0(\chi)$ must be strictly decreasing. Hence, $\frac{\mathrm{d}h_0}{\mathrm{d}\chi}<0$ for $\chi\in\langle\chi_1,\chi_0\rangle$.

From (4.4a) and (4.4b) we further see that the derivative of $h_0(\chi)$ is bounded at the boundary points, $\chi_0$ and $\chi_1$. Thus, since $h_0(\chi)$ is monotone for $\chi\in\langle\chi_1,\chi_0\rangle$, $\frac{\mathrm{d}h_0}{\mathrm{d}\chi}$ will be bounded for all $\chi\in\langle\chi_1,\chi_0\rangle$.

□

### 4.1.3 The Special Case: $\Gamma\to0$

We will now consider the situation of high injection rate $Q_{\text{well}}$ or small differences in density ($\Delta\rho\to0$). It follows that $\Gamma$ becomes so small that we can neglect the terms proportional

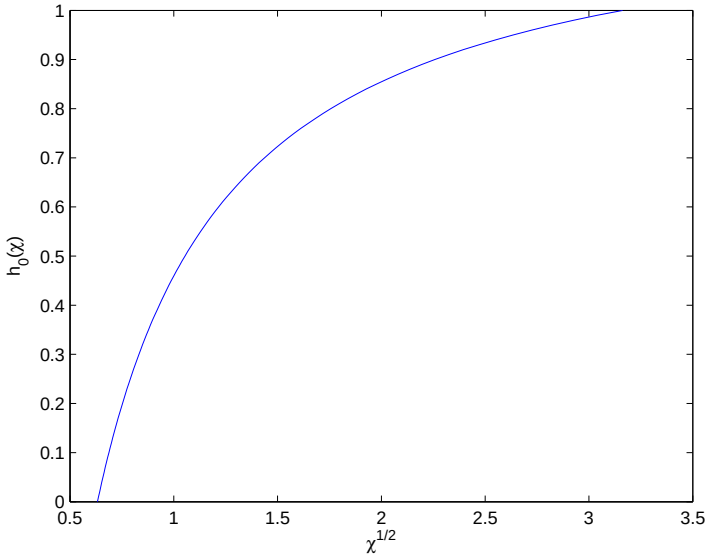


Figure 4.2: The solution $h_0(\chi)$ for the case of $\Gamma \to 0$. Here I have used $\lambda = 5$.

to $\Gamma$. Thus, $\Gamma$ is below $\Gamma_c$, and we have stability. Since we have stability, we consider Equation (4.1) for $h_0(\chi)$. By neglecting all the $\Gamma$-terms in Equation (4.1) we are left with,

$$\chi = \frac{2\lambda}{[1 + (\lambda - 1)h_0]^2} \,. \tag{4.12}$$

This equation can be inverted for $h_0(\chi)$ to give:

$$h_0(\chi) = \begin{cases} 1 & \text{for} \quad \chi < \frac{2}{\lambda} \\ \frac{\sqrt{\frac{2\lambda}{\chi}} - 1}{\lambda - 1} & \text{for} \quad \frac{2}{\lambda} < \chi < 2\lambda \\ 0 & \text{for} \quad \chi > 2\lambda \end{cases} \tag{4.13}$$

By plotting $h_0(\chi)$ as a function of $\chi$, for $\lambda > 1$, we see from Figure 4.2 that it has the same shape as the function in Figure 4.1. Here, $\sqrt{\chi}$ is choosen as the horizontal axis, as it is proportional to the radial distance $r$ (see 3.9). From Equation (4.13) we further observe that $h_0(\chi)$ approaches a vertical line at $\chi = 2$, in the limit as the mobility ratio $\lambda$ approaches 1. That is, when having equal density and mobility, both fluids will flow with equal velocities at every depth.

The derivative of $h_0(\chi)$ can also be computed:

$$\begin{aligned}\frac{\mathrm{d}h_0}{\mathrm{d}\chi} &= \frac{\sqrt{2\lambda}}{\lambda-1}\frac{\mathrm{d}}{\mathrm{d}\chi}\left(\chi^{-\frac{1}{2}}\right)\\ &= -\frac{\sqrt{\lambda}}{\sqrt{2}(\lambda-1)}\chi^{-\frac{3}{2}} \quad \text{for} \quad \frac{2}{\lambda} < \chi < 2\lambda\,.\end{aligned}$$

We observe that the derivative of $h_0$ will be positive for all $\chi > 0$, in the case of $\lambda < 1$. It also has a singularity at $\lambda = 1$. Thus, Equation (4.13) dose not hold, and we will have to solve Equation (4.1) for the case of $\lambda \leq 1$.

## 4.2 Linear Stability

From the non-linear stability proof of Nordbotten and Celia (2006b) (see Appendix B), we know that for small positive values of $\Gamma$ ($0 < \Gamma < \Gamma_c$), the solution $h_0(\chi)$ of Equation (4.1) is stable. Thus, $h'(\chi,\tau)$ will approach the asymptotic solution $h_0(\chi)$, of (4.1), for late times $\tau$. In order to compare these two equations for other values of $\Gamma$, we choose to linearise (3.13).

### 4.2.1 Linearisation

We express the solution $h'(\chi,\tau)$ as a Taylor expansion with respect to time $\tau$:

$$h'(\chi,\tau) = h_0(\chi) + \varepsilon g(\chi,\tau) + \mathcal{O}(\varepsilon^2), \quad \text{where} \quad \varepsilon > 0\,. \tag{4.14}$$

Here, $h_0(\chi)$ represents the solution of the stationary equation (4.1), while $g(\chi,\tau)$ is an arbitrary bounded function. When $h'(\chi,\tau)$ must satisfy the conservation of $CO_2$, we require

$$\varepsilon \int_0^\infty g(\chi,\tau)\mathrm{d}\chi = 0\,.$$

Thus, $h'(\chi,\tau)$ from (4.14) represents a perturbation of $h_0(\chi)$. We will further assume that the parameter $\varepsilon$ is small, and neglect all terms proportional to $\varepsilon^p$, where $p \geq 2$. By neglecting these terms, we are able to obtain a linearised equation for $g(\chi,\tau)$.

We substitute (4.14) into the time-dependent equation (3.13) to obtain

$$\begin{aligned}\varepsilon\tau\frac{\partial g}{\partial \tau}\left(\frac{\mathrm{d}h_0}{\mathrm{d}\chi} + \varepsilon\frac{\partial g}{\partial \chi}\right)^{-1} &= \chi - \frac{\alpha(\chi,\tau)}{[1+(\lambda-1)(h_0+\varepsilon g)]^2}\\ &\quad + \frac{\beta(\chi,\tau)}{1+(\lambda-1)(h_0+\varepsilon g)}\,,\end{aligned} \tag{4.15}$$

where,

$$\begin{aligned}
\alpha(\chi,\tau) &= 2\lambda\left[1+2\Gamma\lambda\chi(h_0+\varepsilon g)\left(\frac{\mathrm{d}h_0}{\mathrm{d}\chi}+\varepsilon\frac{\partial g}{\partial\chi}\right)\right],\\
\beta(\chi,\tau) &= 4\Gamma\lambda\,(1-h_0-\varepsilon g)\left[h_0+\varepsilon g+\chi\left(\frac{\mathrm{d}h_0}{\mathrm{d}\chi}+\varepsilon\frac{\partial g}{\partial\chi}\right)\right.\\
&\quad\left.+\chi(h_0+\varepsilon g)\left(\frac{\mathrm{d}^2h_0}{\mathrm{d}\chi^2}+\varepsilon\frac{\partial^2 g}{\partial\chi^2}\right)\left(\frac{\mathrm{d}h_0}{\mathrm{d}\chi}+\varepsilon\frac{\partial g}{\partial\chi}\right)^{-1}\right].
\end{aligned}$$

We do not want to have any terms inversely proportional to $\varepsilon$, and represent these terms by their Taylor series:

$$\begin{aligned}
f_1(\varepsilon) &\equiv \left(\frac{\mathrm{d}h_0}{\mathrm{d}\chi}+\varepsilon\frac{\partial g}{\partial\chi}\right)^{-1}\\
&= \left(\frac{\mathrm{d}h_0}{\mathrm{d}\chi}\right)^{-1}-\frac{\frac{\partial g}{\partial\chi}}{\left(\frac{\mathrm{d}h_0}{\mathrm{d}\chi}\right)^2}\varepsilon\,, \qquad (4.16)\\
f_2(\varepsilon) &\equiv \frac{1}{[1+(\lambda-1)(h_0+\varepsilon g)]^2}\\
&= \frac{1}{[1+(\lambda-1)h_0]^2}-\frac{2(\lambda-1)g}{[1+(\lambda-1)h_0]^3}\varepsilon\,, \qquad (4.17)\\
f_3(\varepsilon) &\equiv \frac{1-h_0-\varepsilon g}{1+(\lambda-1)(h_0+\varepsilon g)}\\
&= \frac{1-h_0}{1+(\lambda-1)h_0}-\frac{\lambda g}{[1+(\lambda-1)h_0]^2}\varepsilon\,. \qquad (4.18)
\end{aligned}$$

Again the higher order terms of $\varepsilon$ are neglected. By substituting (4.16)-(4.18) back into Equation (4.15), we get

$$\begin{aligned}
\varepsilon\tau\frac{\partial g}{\partial\tau}\left\{\left(\frac{\mathrm{d}h_0}{\mathrm{d}\chi}\right)^{-1}-\varepsilon\frac{\partial g}{\partial\chi}\left(\frac{\mathrm{d}h_0}{\mathrm{d}\chi}\right)^{-2}\right\} =&\\
\chi-\alpha(\chi,\tau)&\left\{\frac{1}{[1+(\lambda-1)h_0]^2}-\frac{2(\lambda-1)g}{[1+(\lambda-1)h_0]^3}\varepsilon\right\}\\
&+\gamma(\chi,\tau)\left\{\frac{1-h_0}{1+(\lambda-1)h_0}-\frac{\lambda g}{[1+(\lambda-1)h_0]^2}\varepsilon\right\},
\end{aligned}$$

where,

$$\begin{aligned}\gamma(\chi,\tau) &= 4\Gamma\lambda\Bigg[h_0+\varepsilon g+\chi\left(\frac{\mathrm{d}h_0}{\mathrm{d}\chi}+\varepsilon\frac{\partial g}{\partial\chi}\right)\\ &\quad+\chi(h_0+\varepsilon g)\left(\frac{\mathrm{d}^2h_0}{\mathrm{d}\chi^2}+\varepsilon\frac{\partial^2 g}{\partial\chi^2}\right)\left\{\left(\frac{\mathrm{d}h_0}{\mathrm{d}\chi}\right)^{-1}-\varepsilon\frac{\partial g}{\partial\chi}\left(\frac{\mathrm{d}h_0}{\mathrm{d}\chi}\right)^{-2}\right\}\Bigg]\,.\end{aligned}$$

Now, all the nonlinear terms are of order $\varepsilon^2$. When considering $\varepsilon$ as small, we neglect these terms and are left with a linear partial differential equation. Furthermore, all terms proportional to $\varepsilon^0$ constitute the right-hand side of (4.1). Thus, these terms add up to zero, and we are only left with the terms proportional to $\varepsilon$. Multiplying both sides by $\varepsilon^{-1}$, we obtain a linear equation for $g(\chi,\tau)$:

$$\frac{\partial g}{\partial\tau}=\frac{4}{\tau}\left[A(\chi)\frac{\partial^2 g}{\partial\chi^2}+B(\chi)\frac{\partial g}{\partial\chi}+C(\chi)g\right]\,, \tag{4.19}$$

where,

$$A(\chi) = \frac{\Gamma\lambda\chi(1-h_0)h_0}{1+(\lambda-1)h_0}\,, \tag{4.20}$$

$$\begin{aligned}B(\chi) &= -\frac{\Gamma\lambda^2\chi h_0\frac{\mathrm{d}h_0}{\mathrm{d}\chi}}{[1+(\lambda-1)h_0]^2}\\ &\quad+\frac{\Gamma\lambda\chi(1-h_0)}{1+(\lambda-1)h_0}\left[\frac{\mathrm{d}h_0}{\mathrm{d}\chi}-h_0\frac{\mathrm{d}^2h_0}{\mathrm{d}\chi^2}\left(\frac{\mathrm{d}h_0}{\mathrm{d}\chi}\right)^{-1}\right]\,,\end{aligned} \tag{4.21}$$

$$\begin{aligned}C(\chi) &= \frac{\lambda(\lambda-1)\frac{\mathrm{d}h_0}{\mathrm{d}\chi}}{[1+(\lambda-1)h_0]^3}\left[1+2\Gamma\lambda\chi h_0\frac{\mathrm{d}h_0}{\mathrm{d}\chi}\right]\\ &\quad-\frac{\Gamma\lambda^2}{[1+(\lambda-1)h_0]^2}\left[h_0\frac{\mathrm{d}h_0}{\mathrm{d}\chi}+2\chi\left(\frac{\mathrm{d}h_0}{\mathrm{d}\chi}\right)^2+\chi h_0\frac{\mathrm{d}^2h_0}{\mathrm{d}\chi^2}\right]\\ &\quad+\frac{\Gamma\lambda(1-h_0)}{1+(\lambda-1)h_0}\left[\frac{\mathrm{d}h_0}{\mathrm{d}\chi}+\chi\frac{\mathrm{d}^2h_0}{\mathrm{d}\chi^2}\right]\,.\end{aligned} \tag{4.22}$$

We want to show that the arbitrary perturbation $g(\chi,\tau)$ in Equation (4.19) approaches zero as $\tau\to\infty$. Thus, if we can show that

$$\frac{\partial}{\partial\tau}[\max_{\chi}|g(\chi,\tau)|]<0\,,$$

for all $\chi\in[\chi_1,\chi_0]$ and $\tau>0$, we have linear stability.

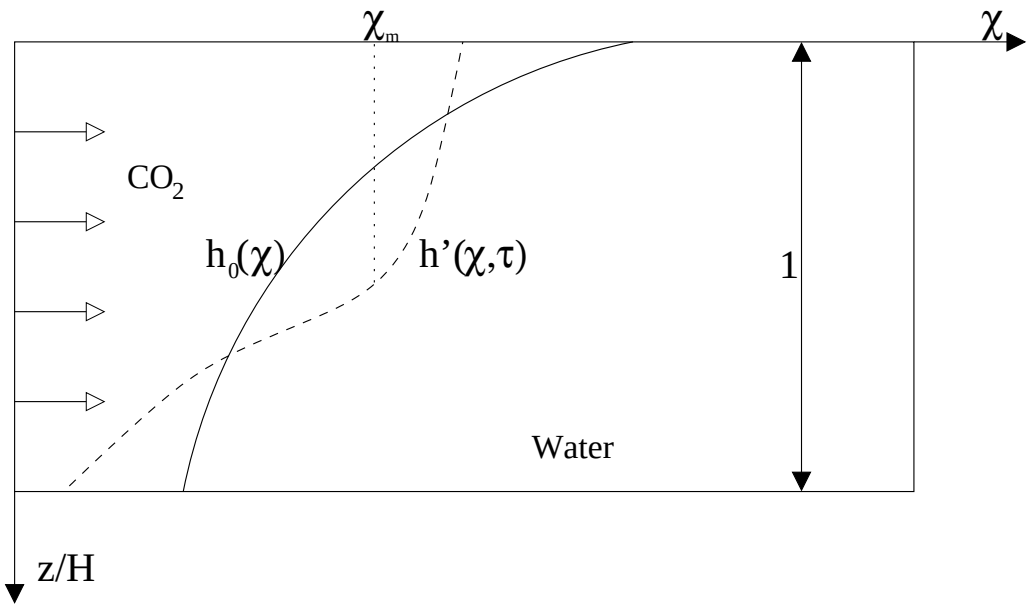


Figure 4.3: $h'(\chi,\tau)$ as a perturbation of $h_0(\chi)$, at a fixed time $\tau$. For illustration purpose, we have chosen the perturbation $\varepsilon$, as quite large in this figure.

### 4.2.2 Stability Analysis

In Figure 4.3, the dotted line represents the perturbated solution $h'(\chi,\tau) = h_0(\chi)+\varepsilon g(\chi,\tau)$, while the continuous line shows the stationary solution $h_0(\chi)$. We define:

$$\chi_m = \{\chi : |g(\chi_m,\tau)| \geq |g(\chi,\tau)|\}\,.$$

We are interested in how the arbitrary perturbation $g(\chi,\tau)$ evolves in time. Evaluated in $\chi_m$, we want to show that

$$h'(\chi_m,\tau) = h_0(\chi_m) + \varepsilon g(\chi_m,\tau) \to h_0(\chi_m)\,, \quad \text{as} \quad \tau \to \infty\,.$$

If we can show that $|g(\chi_m,\tau)|$ is monotonically decreasing as $\tau \to \infty$, this expression will be satisfied, and we will have linear stability.

**Case $0 < \mathbf{h_0}(\chi_\mathbf{m}) < 1$**. Consider first that $g(\chi,\tau)$ has a minimum or maximum at $\chi_m \in \langle\chi_1,\chi_0\rangle$. Thus, $\frac{\partial g}{\partial \chi}|_{\chi_m} = 0$. For the case of $g(\chi_m,\tau) < 0$, we will have $\frac{\partial^2 g}{\partial \chi^2}|_{\chi_m} > 0$. Furthermore (4.20) shows that $A(\chi) \geq 0$ for all $\Gamma$, $\lambda$ and $\chi > 0$. Thus, from (4.19) we have

$$\begin{aligned}\left.\frac{\partial g}{\partial \tau}\right|_{\chi_m} &= \frac{4\varepsilon}{\tau}\left[A(\chi_m)\left.\frac{\partial^2 g}{\partial \chi^2}\right|_{\chi_m} + C(\chi_m)g(\chi_m,\tau)\right] \\ &> 0 \quad \text{for} \quad C(\chi_m) < 0\,.\end{aligned}$$

For the case of $g(\chi_m, \tau) > 0$, we have $\frac{\partial^2 g}{\partial \chi^2}|_{\chi_m} < 0$. Thus,

$$\left.\frac{\partial g}{\partial \tau}\right|_{\chi_m} < 0 \quad \text{for} \quad C(\chi_m) < 0\,.$$

Hence, we need to show that $C(\chi_m) < 0$.

**Case $\mathbf{h_0}(\chi_\mathbf{m}) = \mathbf{0}$.** This is the case of $\chi_m = \chi_0$. From Equation (4.20) and (4.21) we have,

$$A(\chi_0) = 0 \quad \text{and} \quad B(\chi_0) = \Gamma\lambda\chi_0 \left.\frac{\mathrm{d}h_0}{\mathrm{d}\chi}\right|_{\chi_0^-} < 0\,.$$

Also, from (4.22), (4.4a) and (4.5a) we obtain,

$$\begin{aligned}
C(\chi_0) &= \lambda(\lambda-1)\left.\frac{\mathrm{d}h_0}{\mathrm{d}\chi}\right|_{\chi_0^-} - 2\Gamma\lambda^2\chi_0\left(\left.\frac{\mathrm{d}h_0}{\mathrm{d}\chi}\right|_{\chi_0^-}\right)^2 \\
&\quad + \Gamma\lambda\left[\left.\frac{\mathrm{d}h_0}{\mathrm{d}\chi}\right|_{\chi_0^-} + \chi_0\left.\frac{\mathrm{d}^2h_0}{\mathrm{d}\chi^2}\right|_{\chi_0^-}\right] \\
&= \frac{(\lambda-1)(2\lambda-\chi_0)}{4\Gamma\chi_0} - \frac{4\lambda^2 - 4\lambda\chi_0 + \chi_0^2}{8\Gamma\chi_0} + \frac{2\lambda-\chi_0}{4\chi_0} \\
&\quad + \frac{\chi_0^2 - 2\chi_0 + 2\Gamma\chi_0 - 2\lambda\chi_0 - 8\Gamma\lambda + 4\lambda}{16\Gamma\chi_0} \\
&= \frac{1}{16\Gamma\chi_0}(8\lambda^2 - 4\lambda\chi_0 - 8\lambda + 4\chi_0 - 8\lambda^2 + 8\lambda\chi_0 - 2\chi_0^2 + 8\Gamma\lambda \\
&\quad - 4\Gamma\chi_0 + \chi_0^2 - 2\chi_0 + 2\Gamma\chi_0 - 2\lambda\chi_0 - 8\Gamma\lambda + 4\lambda) \\
&= \frac{1}{16\Gamma\chi_0}\left(2\lambda\chi_0 - 4\lambda + 2\chi_0 - \chi_0^2 - 2\Gamma\chi_0\right) \\
&= \frac{1}{16\Gamma\chi_0}\left[(2-\chi_0)(\chi_0 - 2\lambda) - 2\Gamma\chi_0\right]\,.
\end{aligned}$$

Since we have proved $\frac{\mathrm{d}h_0}{\mathrm{d}\chi} < 0$ for $\chi \in \langle \chi_1, \chi_0 \rangle$, Equation (4.4a) implies $\chi_0 > 2\lambda$. Also, from the volume condition (4.8), we have $\chi_0 > 2$. Thus, $C(\chi_0) < 0$. Furthermore, since $h_0(\chi, \tau) \geq 0$, we must have $g(\chi_0, \tau) \geq 0$. This implies $\frac{\partial g}{\partial \chi}|_{\chi_m} \geq 0$. Hence, from Equation (4.19) we obtain,

$$\left.\frac{\partial g}{\partial \tau}\right|_{\chi_m} = \frac{4\varepsilon}{\tau}\left[B(\chi_m)\left.\frac{\partial g}{\partial \chi}\right|_{\chi_m} + C(\chi_m)g(\chi_m, \tau)\right] < 0\,,$$

for all $\tau > 0$.

**Case $\mathbf{h_0(\chi_m) = 1}$.** This is the case of $g(\chi_m, \tau)$ having a minimum at the boundary $\chi_1$. From (4.20) and (4.21) we get,

$$A(\chi_1) = 0 \quad \text{and} \quad B(\chi_1) = -\Gamma\chi_1 \frac{\mathrm{d}h_0}{\mathrm{d}\chi}\bigg|_{\chi_1^+} > 0 \,.$$

From (4.22), (4.4b) and (4.5b) we can get an expression for $C(\chi_1)$:

$$\begin{aligned}
C(\chi_1) &= \left(\frac{\lambda-1}{\lambda^2}\right)\frac{\mathrm{d}h_0}{\mathrm{d}\chi}\bigg|_{\chi_1^+} + \frac{2\Gamma(\lambda-1)}{\lambda}\chi_1\left(\frac{\mathrm{d}h_0}{\mathrm{d}\chi}\bigg|_{\chi_1^+}\right)^2 \\
&\quad -\Gamma\left[\frac{\mathrm{d}h_0}{\mathrm{d}\chi}\bigg|_{\chi_1^+} + 2\chi_1\left(\frac{\mathrm{d}h_0}{\mathrm{d}\chi}\bigg|_{\chi_1^+}\right)^2 + \chi_1\frac{\mathrm{d}^2h_0}{\mathrm{d}\chi^2}\bigg|_{\chi_1^+}\right] \\
&= \left(\frac{\lambda-1}{\lambda^2}-\Gamma\right)\frac{\mathrm{d}h_0}{\mathrm{d}\chi}\bigg|_{\chi_1^+} - \frac{2\Gamma\chi_1}{\lambda}\left(\frac{\mathrm{d}h_0}{\mathrm{d}\chi}\bigg|_{\chi_1^+}\right)^2 - \Gamma\chi_1\frac{\mathrm{d}^2h_0}{\mathrm{d}\chi^2}\bigg|_{\chi_1^+} \\
&= \left(\frac{\lambda-1}{\lambda^2}-\Gamma\right)\frac{\mathrm{d}h_0}{\mathrm{d}\chi}\bigg|_{\chi_1^+} - \frac{2\Gamma\chi_1}{\lambda}\left(\frac{\mathrm{d}h_0}{\mathrm{d}\chi}\bigg|_{\chi_1^+}\right)^2 \\
&\quad +\frac{\Gamma\chi_1}{\lambda}\left(\frac{\mathrm{d}h_0}{\mathrm{d}\chi}\bigg|_{\chi_1^+}\right)^2 + \left(\Gamma - \frac{\lambda-1}{2\lambda^2}\right)\frac{\mathrm{d}h_0}{\mathrm{d}\chi}\bigg|_{\chi_1^+} - \frac{1}{8} \\
&= -\frac{\Gamma\chi_1}{\lambda}\left(\frac{\mathrm{d}h_0}{\mathrm{d}\chi}\bigg|_{\chi_1^+}\right)^2 + \left(\frac{\lambda-1}{2\lambda^2}\right)\frac{\mathrm{d}h_0}{\mathrm{d}\chi}\bigg|_{\chi_1^+} - \frac{1}{8} \\
&= \left(\frac{\lambda-1}{2\lambda^2}\right)\frac{\mathrm{d}h_0}{\mathrm{d}\chi}\bigg|_{\chi_1^+} - \left(\frac{\lambda\chi_1-2}{4\lambda^2}\right)\frac{\mathrm{d}h_0}{\mathrm{d}\chi}\bigg|_{\chi_1^+} - \frac{1}{8} \\
&= \left(\frac{2-\chi_1}{4\lambda}\right)\frac{\mathrm{d}h_0}{\mathrm{d}\chi}\bigg|_{\chi_1^+} - \frac{1}{8} \,.
\end{aligned}$$

Since $\chi_1 < \chi_0$, the volume condition (4.8), requires $\chi_1 \leq 2$. From Theorem 4.1.1 we have $\frac{\mathrm{d}h_0}{\mathrm{d}\chi} < 0$ for $\chi \in \langle \chi_1, \chi_0 \rangle$. Thus, $C(\chi_1) < 0$. Furthermore, when $\chi_m = \chi_1$, $g(\chi_m, \tau)$ has a minimum at the left boundary point (see Figure 4.3). Thus, $\frac{\partial g}{\partial \chi}|_{\chi_1^+} \geq 0$, and from (4.19) we obtain,

$$\frac{\partial g}{\partial \tau}\bigg|_{\chi_m} = \frac{4\varepsilon}{\tau}\left[B(\chi_m)\frac{\partial g}{\partial \chi}\bigg|_{\chi_m} + C(\chi_m)g(\chi_m,\tau)\right] > 0 \,,$$

for all $\tau > 0$.

## 4.3 Summary

By linearising the solution $h'(\chi,\tau) = h_0(\chi) + \varepsilon g(\chi,\tau)$, we were able to compare the two equations, (3.14) and (3.13), from the previous chapter. From the linear analysis, we carried out a linear second order partial differential equation for $g(\chi,\tau)$, with coefficients dependent upon the solution $h_0(\chi)$ and $\frac{\mathrm{d}h_0(\chi)}{\mathrm{d}\chi}$, from the stationary equation.

When studying the stationary equation (4.1), we found expressions for the first and second derivative of $h_0(\chi)$, at the boundaries. We also proved that the first derivative of $h_0(\chi)$ is monotone and less than zero, for $\chi_1 < \chi < \chi_0$. From these properties of the stationary equation, we were able to carry out a criterion on the linear stability. That is, $C(\chi) < 0$, where $C(\chi)$ is given by (4.22). Furthermore, we showed that this criterion was satisfied on the boundary.

Numerically, we can solve the stationary equation (4.1). Since the variable $C(\chi)$ is dependent upon this solution $h_0(\chi)$, and the first and second derivative of $h_0(\chi)$, we can solve for $C(\chi)$ numerically. We also derived an expression for the conservation of $CO_2$ in self-similar coordinates. This will become useful in the numerical implementation. The numerical analysis is presented in the next chapter.

# Chapter 5

# Numerical Results

The stationary equation (4.1) discussed in the previous chapter can be solved numerically, by means of for example a Runge-Kutta method. By solving for $h_0(\chi)$, $\frac{\mathrm{d}h_0}{\mathrm{d}\chi}$ and $\frac{\mathrm{d}^2h_0}{\mathrm{d}\chi^2}$, we can compute the value of $C(\chi)$ and analyse the linear stability, discussed in the previous chapter. By solving $C(\chi)$ for different values of $\Gamma$ and $\lambda$ we will investigate the region of linear stability. We will also compute $\Gamma_c$ for different values of $\lambda$, and find the region of stability for the non-linear stability analysis of Nordbotten and Celia (2006b). When solving the time-dependent equation numerically, we will further discuss the range of these stability results.

## 5.1 The Runge-Kutta Method

We will consider the following initial value problem:

$$\frac{\mathrm{d}y}{\mathrm{d}t} = f(t, y), \quad y(t_0) = y_0 \,. \tag{5.1}$$

Many numerical methods are developed, for solving these kind of problems. We will consider the method of Runge-Kutta, which is a Taylor series method. The theory presented in this chapter is based on (Cheney and Kincaid 2002).

The Taylor series is given by

$$y(t_0 + \Delta t) = y(t_0) + \Delta t \frac{\mathrm{d}}{\mathrm{d}t} y(t_0) + \frac{1}{2}(\Delta t)^2 \frac{\mathrm{d}^2}{\mathrm{d}t^2} y(t_0) + ... \tag{5.2}$$

By using a finite part of this series, we can compute the needed number of derivatives of $f(t, y)$ and find an approximation to $y(t_0 + \Delta t)$ from the initial value of $y_0$. In the same manner, we can compute $y(t_0 + i\Delta t)$ at step $i$. Thus, we can solve Equation (5.1) on a finite interval $I$. The step length $\Delta t$, need not be fixed. A Taylor series method that uses $n$ terms of the Taylor series, is said to be of order $n$. The local truncation error of this method is then given by

$$E_n = \frac{1}{(n+1)!}(\Delta t)^{n+1}\frac{\mathrm{d}^{n+1}}{\mathrm{d}t^{n+1}}y(t+\theta\Delta t), \quad \text{when} \quad 0<\theta<1\,.$$

A standard Taylor series method requires analytical expressions for $f(t,y)$ and the derivatives of $f(t,y)$. However, for some expressions of $f(t,y)$, possibly non-linear, the derivatives of $f(t,y)$ might be difficult to compute. The Runge-Kutta methods manage to avoid the calculation of the derivatives of $f(t,y)$.

Consider the differentiation of Equation (5.1),

$$\begin{aligned}\frac{\mathrm{d}^2y}{\mathrm{d}t^2} &= \frac{\partial f}{\partial t}+\frac{\partial f}{\partial y}\frac{\mathrm{d}y}{\mathrm{d}t}\\ &= \frac{\partial f}{\partial t}+f\frac{\partial f}{\partial y}\,.\end{aligned}$$

By substituting this expression into (5.2), we obtain

$$\begin{aligned}y(t_0+\Delta t) &= y(t_0)+\Delta t f(t,y)+\frac{1}{2}(\Delta t)^2[\frac{\partial}{\partial t}f(t,y)+f(t,y)\frac{\partial}{\partial y}f(t,y)]+\mathcal{O}((\Delta t)^3)\\ &= y(t_0)+\frac{1}{2}\Delta t f(t,y)+\frac{1}{2}\Delta t f(t+\Delta t, y+\Delta t f(t,y))+\mathcal{O}((\Delta t)^3)\,, \qquad (5.3)\end{aligned}$$

where $f(t+\Delta t, y+\Delta t f(t,y))$ is given by its Taylor series. When neglecting the higher order terms, this becomes a second order Runge-Kutta method. We see from Equation (5.3), that we do not need to calculate any derivatives of $f(t,y)$. Higher order Runge-Kutta methods can be derived in the same manner. The fourth order Runge-Kutta method, also called the classical Runge-Kutta method, is given by

$$y(t+\Delta t) = y(t)+\frac{1}{6}(F_1+2F_2+2F_3+F_4)\,,$$

where

$$\begin{aligned}F_1 &= \Delta t f(t,y)\,,\\ F_2 &= \Delta t f(t+\frac{1}{2}\Delta t, y+\frac{1}{2}F_1)\,,\\ F_3 &= \Delta t f(t+\frac{1}{2}\Delta t, y+\frac{1}{2}F_2)\,,\\ F_4 &= \Delta t f(t+\Delta t, y+F_3)\,.\end{aligned}$$

This is the most frequently used Runge-Kutta method. Higher order methods are more accurate, but also more expensive to use. The truncation error for this fourth order method will be of order $(\Delta t)^5$, since it only uses the first four terms of the Taylor series (5.2). It is however difficult to derive an exact expression for this error.

### 5.1.1 Adaptive Runge-Kutta Method

For efficiency, we do not want the step size $\Delta t$ to be too small. In order to choose a reasonable value for this step size, we need a method which also solves for the error in each step. An adaptive method adjusts the step size $\Delta t$ in every step, keeping the error bounded within some specified interval.

In our numerical implementation in Matlab, we have used the function ode45. This is a Runge-Kutta-Fehlberg method, which uses an additional fifth order Runge-Kutta method, in order to calculate for the error in every step. The fifth order Runge-Kutta method uses the same evaluation points as the fourth order method; a total of six evaluation points (Hairer et al. 1987).

By solving the value of $y(t + \Delta t)$ twice, the method compares the two solutions, and gets an estimate for the error. If the difference is small, we may choose to make the step size $\Delta t$ larger for the next calculation. If the difference is larger than some tolerance, we make the step size, $\Delta t$, smaller, and recomputes $y(t + \Delta t)$.

## 5.2 The Numerical Model

Equation (4.1) is a second order ordinary differential equation for $h_0(\chi)$. By the transformation,

$$f_1 = h_0 \quad \text{and} \quad f_2 = \frac{\mathrm{d}h_0}{\mathrm{d}\chi}\,,\,, \tag{5.4}$$

we can transform the equation to a system of two first order equations. That is,

$$\frac{\mathrm{d}f_1}{\mathrm{d}\chi} = f_2\,, \tag{5.5}$$

$$\frac{\mathrm{d}f_2}{\mathrm{d}\chi} = \frac{(1+(\lambda-1)f_1)f_2}{4\Gamma\lambda\chi f_1(1-f_1)}\left[\frac{2\lambda\,(1+2\Gamma\lambda\chi f_1 f_2)}{[1+(\lambda-1)f_1]^2} - \chi - 4\Gamma\lambda\frac{1-f_1}{1+(\lambda-1)f_1}\,(f_1+\chi f_2)\right]. \tag{5.6}$$

These equations are on the same form as Equation (5.1), and can be solved by means of Runge-Kutta methods, if we can specify some initial conditions.

We are interested in solving for $h_0 \in [0,1]$. Thus, from (5.4), (4.2) and (4.4a), the initial conditions should be,

$$f_1(\chi_0) = 0 \quad \text{and} \quad f_2(\chi_0^-) = \frac{\mathrm{d}h_0(\chi_0^-)}{\mathrm{d}\chi} = \frac{2\lambda-\chi_0}{4\Gamma\lambda\chi_0}\,.$$

However, Equation (4.1) degenerates at $h_0(\chi_0) = 0$. Also, from (5.6), we see that $\frac{\mathrm{d}f_2}{\mathrm{d}\chi}$ has a singularity at this point. Hence, we will have to choose the initial condition for Equation (5.5) at some neighbourhood $\chi_\varepsilon$, where

$$h_0(\chi_\varepsilon) = \varepsilon \,. \tag{5.7}$$

By use of the Taylor series, we can write

$$\chi_\varepsilon = \chi_0 + \varepsilon \left( \frac{\mathrm{d}h_0}{\mathrm{d}\chi}\bigg|_{\chi_0^-} \right)^{-1} = \chi_0 + \frac{4\Gamma\lambda\chi_0\varepsilon}{2\lambda - \chi_0} \,.$$

Using the Taylor series again, we can also write the initial condition for Equation (5.6),

$$\begin{aligned} \frac{\mathrm{d}h_0}{\mathrm{d}\chi}\bigg|_{\chi_\varepsilon} &= \frac{\mathrm{d}h_0}{\mathrm{d}\chi}\bigg|_{\chi_0^-} + (\chi_\varepsilon - \chi_0)\frac{\mathrm{d}^2h_0}{\mathrm{d}\chi^2}\bigg|_{\chi_0^-} \\ &= \frac{1}{4\Gamma\lambda\chi_0}\Bigg[2\lambda - \chi_0 + \frac{\lambda\varepsilon}{2\lambda - \chi_0}(\chi_0^2 - 2\chi_0 \\ &\quad +2\Gamma\chi_0 - 2\lambda\chi_0 - 8\Gamma\lambda + 4\lambda)\Bigg] \,. \end{aligned} \tag{5.8}$$

Here the second derivative of $h_0(\chi)$ is given by (4.5a). Now, we have two initial conditions, (5.7) and (5.8). Thus, we can solve Equation (5.5) and (5.6) numerically by a Runge-Kutta method.

The numerical implementation is done in Matlab, using the ode45 routine. When we do not know the value of the point $\chi_0$, we will have to make a guess. For a given starting value $\chi_0$, we can compute $\chi_\varepsilon$ and $\frac{\mathrm{d}h_0(\chi_\varepsilon)}{\mathrm{d}\chi}$ and solve Equation (5.5) and (5.6) for chosen values of $\Gamma$ and $\lambda$. By integrating the solution from 0 to $\chi_0$, the solution must further satisfy the conservation of $CO_2$, given by (4.8). By an iterative solver, we choose new starting points until we get a small enough error for the condition of (4.8).

## 5.3 Results

In Figure (5.1), we have plotted the solutions of $h_0(\chi)$ for $\lambda = 15$ and $\Gamma = 0.5$, 2.5 and 10. We see that more $CO_2$ is flowing on top of the water phase in the case of $\Gamma = 10$, than in the case of $\Gamma = 2.5$ and $\Gamma = 0.5$. The horizontal axis is here represented by $\sqrt{\chi}$, where

$$\chi = \frac{\eta^2}{\tau} = \frac{2\pi r^2 H\phi(1 - S_{res})}{Q_{\text{well}}t} \,. \tag{5.9}$$

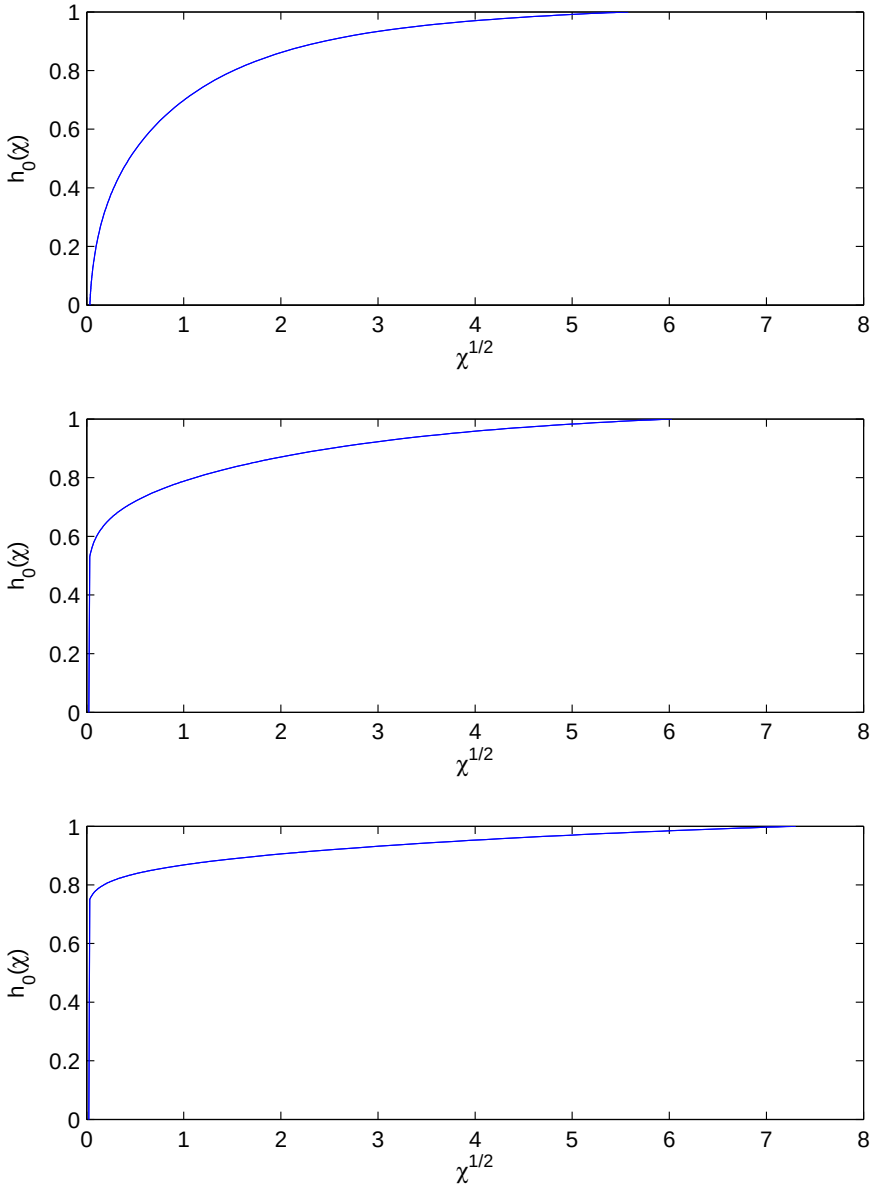


Figure 5.1: The three plots shows the spatial distribution of the $CO_2$ phase, for the case $\Gamma = 0.5$, 2.5 and 10, taken from the top. In all three plots we have used $\lambda = 15$. We see that more $CO_2$ is flowing on top of the water phase for $\Gamma = 10$, than for $\Gamma = 0.5$ and 2.5.

We see from (5.9) that $\sqrt{\chi}$ is proportional with $r$. Typical values for the spatial distribution of the $CO_2$ phase in an aquifer is further calculated in Table 5.1 below. Here $r$ is the number of meters, $\chi = 1$ represents, for $t_1 = 24$ hours and $t_2 = 1$ year. The parameter $H$, denotes

| Sites | $H$ (m) | $\phi$ (%) | $Q_{\text{well}}$ (Mt/y) | $\rho_c$ (kg/m$^3$) | $k$ (mD) | $\Gamma$ (1) | $r$ (m) $t_1$ | $t_2$ |
|---|---|---|---|---|---|---|---|---|
| Utsira | 200 | 35 | 1 | 500 | 2000 | 70.68 | 4.99 | 95.37 |
| Alberta | 50 | 10 | 1 | 500 | 10 | 0.022 | 18.68 | 356.82 |

Table 5.1: The table shows geological data from two different aquifers. Here $H$ denotes the thickness, $\phi$ is the porosity, $Q_{\text{well}}$ the injection rate, $\rho_c$ the $CO_2$ density and $k$ the horizontal permability, associated with each of the aquifers. The dimensionless parameter $\Gamma$ is also calculated in both cases. The spatial variable $r$, is computed from (5.9), when $\chi = 1$ and $t = t_1 = 24$ hours and $t_2 = 1$ year.

the thickness of the aquifer. In this table we have collected data for two different aquifers. The Utsira formation, is located in the North Sea. Statoil is currently injecting 1 megaton of $CO_2$ per year, into this formation, approximately 1000 meters below the bottom of the sea. The data for the Utsira formation is based on Lindeberg (2003). The other aquifer is located in Alberta, Canada. As a possible storage site for $CO_2$, much research has been conducted for the purpose of collecting geological data for this aquifer. Here, we have based our data on Nordbotten and Celia (2006a). While Utsira is a high-permeable sand formation, the Alberta basin has both lower permability and porosity. The large difference in $\Gamma$, is related to this large difference in the permability $k$, and the variation in thickness $H$. The fluid parameters are chosen to be equal, in both aquifers. The value of these fluid parameters are based upon the data from Nordbotten and Celia (2006a). Since these values vary with both the temperature and the depth of the aquifer, we have chosen to use some averaged values. We have used: $\rho_c = 500$ kg, $\Delta\rho = 600$ kg and $\lambda_w = 0.66$ mPa/s. Also, $S_{\text{res}} = 0.5$ and $Q_{\text{well}} = 1$ Mt/y, is used in both cases.

### 5.3.1 Non-Linear Stability

The non-linear stability analysis of Nordbotten and Celia (2006b) shows stability for $\Gamma < \Gamma_c(\lambda)$ (see Appendix B). That is, for

$$1 - \Gamma\left[\frac{4\lambda}{1+(\lambda-1)h_0}\left(\frac{\lambda h_0}{1+(\lambda-1)h_0} - (1-h_0)\right)\frac{\mathrm{d}h_0}{\mathrm{d}\chi} - \frac{4\lambda h_0(1-h_0)}{1+(\lambda-1)h_0}\left(\frac{\mathrm{d}h_0}{\mathrm{d}\chi}\right)^{-1}\frac{\mathrm{d}^2h_0}{\mathrm{d}\chi^2}\right] > 0\,. \quad (5.10)$$

When solving Equation (5.5) and (5.6) by a Runge-Kutta-Fehlberg method, using the initial conditions of (5.7) and (5.8), we can find the values of $h_0$, $\frac{\mathrm{d}h_0}{\mathrm{d}\chi}$ and $\frac{\mathrm{d}^2h_0}{\mathrm{d}\chi^2}$ at $\chi_i \in \langle\chi_1, \chi_0\rangle$, for different values of $\Gamma$ and $\lambda$. These, we can use in Equation (5.10) to compute the values of $\Gamma_c(\lambda)$ (see Figure 5.2).

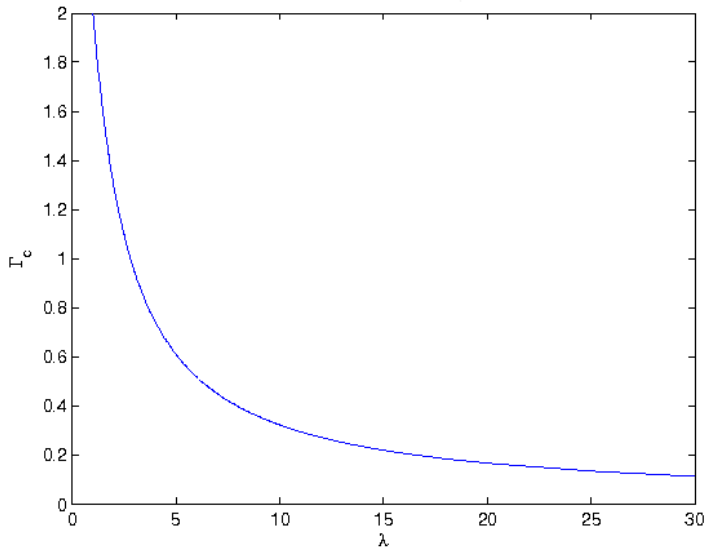


Figure 5.2: $\Gamma_c$ as a function of $\lambda$. We have stability in the region below this curve.

### 5.3.2 Linear Stability

In the previous chapter we showed that the linearised solution, $h'(\chi,\tau) = h_0(\chi) + \varepsilon g(\chi,\tau)$, is stable for

$$C(\chi) = \frac{\lambda(\lambda-1)\frac{\mathrm{d}h_0}{\mathrm{d}\chi}}{[1+(\lambda-1)h_0]^3}\left[1+2\Gamma\lambda\chi h_0\frac{\mathrm{d}h_0}{\mathrm{d}\chi}\right] - \frac{\Gamma\lambda^2}{[1+(\lambda-1)h_0]^2}\left[h_0\frac{\mathrm{d}h_0}{\mathrm{d}\chi}+2\chi\left(\frac{\mathrm{d}h_0}{\mathrm{d}\chi}\right)^2+\chi h_0\frac{\mathrm{d}^2h_0}{\mathrm{d}\chi^2}\right] + \frac{\Gamma\lambda(1-h_0)}{1+(\lambda-1)h_0}\left[\frac{\mathrm{d}h_0}{\mathrm{d}\chi}+\chi\frac{\mathrm{d}^2h_0}{\mathrm{d}\chi^2}\right] < 0\,. \quad (5.11)$$

Our analysis shows that $C(\chi) < 0$ on the boundaries, $\chi_0$ and $\chi_1$. For the case of $\chi_1 < \chi < \chi_0$, we were not able to prove inequality (5.11). Alternatively, we will evaluate $C(\chi)$ numerically. By solving Equation (5.5) and (5.6) numerically, we can find $h_0(\chi_i)$, $\frac{\mathrm{d}h_0(\chi_i)}{\mathrm{d}\chi}$ and $\frac{\mathrm{d}^2h_0(\chi_i)}{\mathrm{d}\chi^2}$ for $\chi_i \in \langle\chi_1,\chi_0\rangle$ and specified values of $\Gamma$ and $\lambda$. When substituting these results into (4.22), we also find the values for $C(\chi_i)$. We define

$$C_m = \max_{\chi} C(\chi)\,, \quad \text{for} \quad \chi_1 < \chi < \chi_0\,. \quad (5.12)$$

In Figure 5.3 and Figure 5.4 we have plotted $C_m$ as a function of $\Gamma$ and $\lambda$. These numerical results indicates that $C_m$ and thus $C(\chi)$ is everywhere negative. Typical values for the

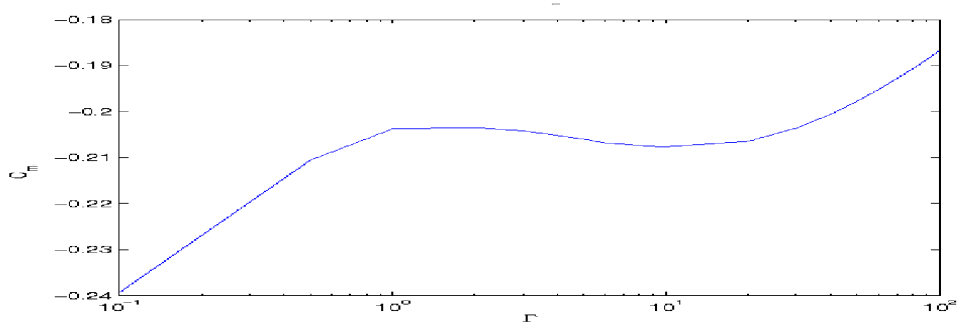


Figure 5.3: $C_m$ (max($C(\chi)$)) as a function of $\Gamma$, when $\lambda = 15$.

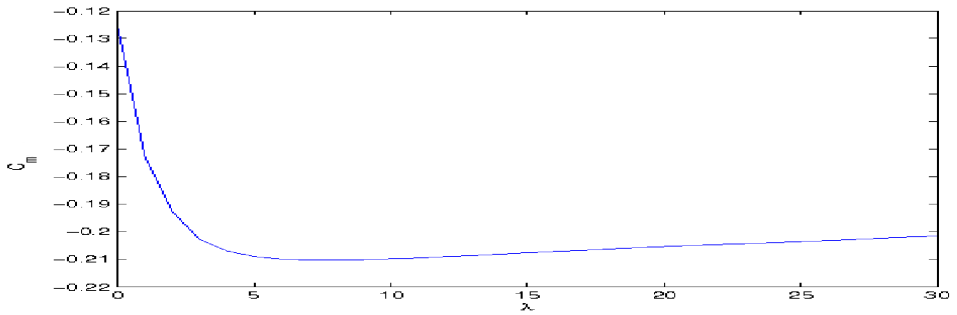


Figure 5.4: $C_m$ (max($C(\chi)$)) as a function of $\lambda$, when $\Gamma = 10$.

mobility ratio, $\lambda$, lie between 5 and 25, dependent upon the depth of the aquifer and the temperature of the fluids. The parameter $\Gamma$ is a more complicated variable, since it depends on several variables and parameters (see (3.9)). For some injection processes it may be of order $10^{-2}$ (Nordbotten and Celia 2006a), and stay below $\Gamma_c$ (from the non-linear stability analysis). In other processes, like on Utsira (Table 5.1), $\Gamma$ may be of order $10^2$. In Figure 5.3 we plotted $\Gamma$ on a logarithmic scale, while $\lambda = 15$ was held fixed. Also, in Figure 5.4 we plotted $C_m$ as a function of the mobility ratio $\lambda$, where $\Gamma = 10$ was held fixed.

## 5.4 Numerical Solution of the Time-Dependent Equation

The time-dependent equation (3.13) is given by,

$$\tau \frac{\partial h'}{\partial \tau}\left(\frac{\partial h'}{\partial \chi}\right)^{-1} = \chi - \frac{2\lambda}{[1+(\lambda-1)h']^2}\left(1 + 2\Gamma\lambda\chi h'\frac{\partial h'}{\partial \chi}\right) + 4\Gamma\lambda\frac{1-h'}{1+(\lambda-1)h'}\left[h' + \chi\frac{\partial h'}{\partial \chi} + \chi h'\frac{\partial^2 h'}{\partial \chi^2}\left(\frac{\partial h'}{\partial \chi}\right)^{-1}\right], \tag{5.13}$$

where $h' = h'(\chi, \tau)$. This equation, we can solve numerically by means of a finite difference method. By solving the non-linear time-dependent equation for different discretisations in $\tau$, we will look at the relative importance of the linear and non-linear terms of $h'(\chi, \tau)$.

We assume the solution $h'(\chi, \tau)$, to be monotone in $\langle 0, 1\rangle$, where

$$\frac{\partial h'}{\partial \chi} < 0 \quad \text{for} \quad \tau > 0\,.$$

Thus, from the inverse function theorem, we can find an inverse function $\chi = \chi(h', \tau)$ (Apostol 1969). By substituting $\frac{\partial h'}{\partial \tau} = \frac{\partial h'}{\partial \chi}\frac{\partial \chi}{\partial \tau}$ on the left side of Equation (5.13), we can write the equation as

$$\frac{\partial \chi}{\partial \tau} = \frac{1}{\tau} F\left(\chi, h', \frac{\partial h'}{\partial \chi}, \frac{\partial^2 h'}{\partial \chi^2}; \Gamma, \lambda\right)\,, \tag{5.14}$$

where $F$ represents the right-hand side of Equation (5.13). By discretising Equation (5.14) in $h' \in [0, 1]$ and $\tau$, we get an explicit method, solving for $\chi_{n,i+1}$:

$$\frac{\chi_{n,i+1} - \chi_{n,i}}{\Delta\tau} = \frac{1}{\tau_i} F_{i,n}\left(\chi, h', \frac{\partial h'}{\partial \chi}, \frac{\partial^2 h'}{\partial \chi^2}; \Gamma, \lambda\right)\,. \tag{5.15}$$

Thus, for an initial value $\chi_{n,0}$, we can solve $\chi_{n,i}$ in time step $i$, for every $h'_n$. For the special case of $\Gamma \to 0$, we have derived an analytical expression for the solution $h_0(\chi)$ of Equation (4.1). Since the derivative of $h_0(\chi)$ is proved to be monotone for $\lambda > 1$ in Theorem 4.1.1, there exists a unique inverse function. Thus, we use expression (4.12) as the initial conditions for our numerical method. Hence, $\chi_{n,0}$ is given by

$$\chi_{n,0} = \frac{2\lambda}{[1 + (\lambda - 1)h'_n]^2}\,. \tag{5.16}$$

Now, we can solve (5.15) for different values of $\Gamma > 0$ and $\lambda > 1$. By choosing $\Gamma < \Gamma_c(\lambda)$, the stability analysis of Nordbotten and Celia (2006b) is ensured, and we expect the solution $h'(\chi, \tau)$ to approach the steady-state solution $h_0(\chi)$.

In Figure 5.5 we have solved Equation (5.15) for $\Gamma = 0.2$, $\lambda = 5$ and timestep $\Delta\tau = 10^{-4}$. From Figure 5.2 we see that this choice of $\Gamma$ and $\lambda$ is within the region of stability. Starting at $\chi_{n,0}$, given by (5.16), we see that the solution approaches the steady-state solution as the number of timesteps increases. Hence, it is stable.

The timestep can be optimised. Since the right-hand side of (5.15) is scaled by $\tau^{-1}$, we can optimise the timestep in every step $i$, such that the fraction $\frac{\Delta\tau}{\tau}$ stays constant. By starting at $\tau_0 = 1$, we thus get

$$\tau_i = \tau_{i-1}(1 + \Delta\tau) = (1 + \Delta\tau)^i\,. \tag{5.17}$$

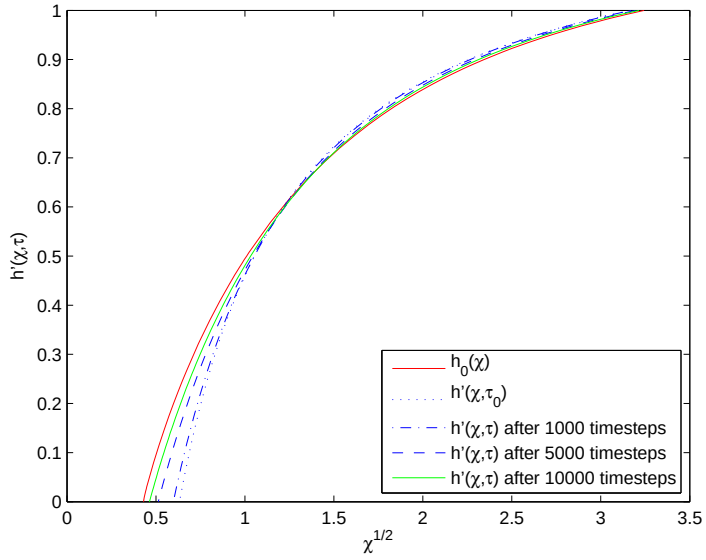


Figure 5.5: The solution $h'(\chi, \tau)$, approaches the steady-state solution $h_0(\chi)$, when $\Gamma = 0.2$ and $\lambda = 5$. Here we have used timestep $\Delta\tau = 10^{-4}$.

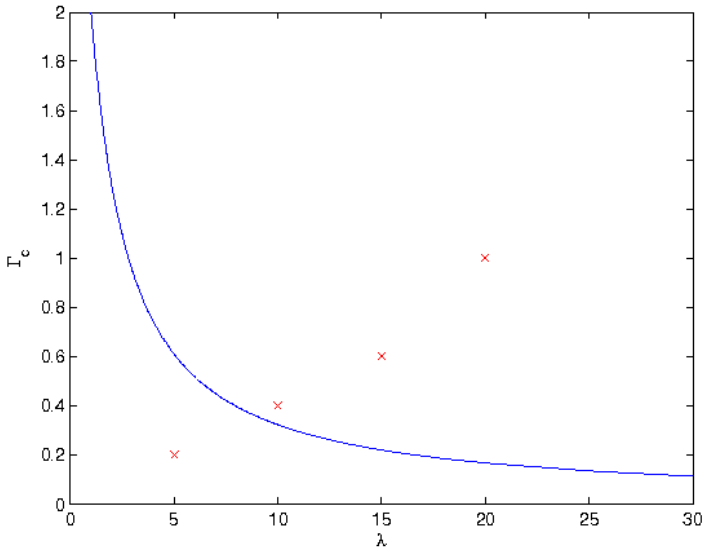


Figure 5.6: We have investigated these four cases, marked at the figure. The left mark is within the region of stability. Thus, we expect $h'(\chi, \tau)$ to approach $h'(\chi)$ as $\tau \to \infty$. The other marks are outside of this region, meaning that we have no information about the stability of these cases.

Furthermore, we have tried to solve (5.15) for the case of $(\Gamma, \lambda) = (0.4, 10), (0.6, 15)$ and

$(1, 20)$, marked in Figure 5.6. The left mark is here the case of $\Gamma = 0.2$ and $\lambda = 5$, which we studied above, and solved for in Figure 5.5. These parameter values was taken within the region of stability. The other three marks are outside of this region, in which case we have no information about the stability.

For the case of $(\Gamma, \lambda) = (0.4, 10)$, we are slightly outside of the region of stability (5.6). When solving (5.15), with $\Delta\tau = 10^{-4}$ (Figure 5.7(a)), we see that the solution still is stable. However, by increasing the step size to $\Delta\tau = 5 \cdot 10^{-4}$, we see that we get an instability after only 1000 timesteps. When increasing the step size by a factor 5, we have also lowered the number of timesteps by a factor 5. The time-span will then be approximately the same, using the recursive formula of (5.17).

Moving to $(\Gamma, \lambda) = (0.6, 15)$, we get instability for $\Delta\tau = 10^{-4}$ (see Figure 5.7(d)). When choosing half the step size, the linear term gets more influence. Thus, we observe from Figure 5.7(c) that we get stability. As the last example, we try to solve Equation (5.15), for $\Gamma = 1$ and $\lambda = 20$. In this case we even get instability for $\Delta\tau = 10^{-5}$.

These experiments indicate that the region of stability, for the non-linear stability analysis of Nordbotten and Celia (2006b) could be extended. When choosing $\Gamma = 0.6$ and $\lambda = 15$, Figure 5.7(c) showed that $h'(\chi, \tau)$ approaches $h_0(\chi)$ for $\Gamma > 2 \cdot \Gamma_c$. As we continue to increase the value of $\Gamma$, we have to choose smaller time steps $\Delta\tau$. Also, since the initial condition is based upon the steady-state solution for the case of $\Gamma = 0$, the initial condition moves farther away from the solution we are seeking. Thus, linear stability may not be enough.

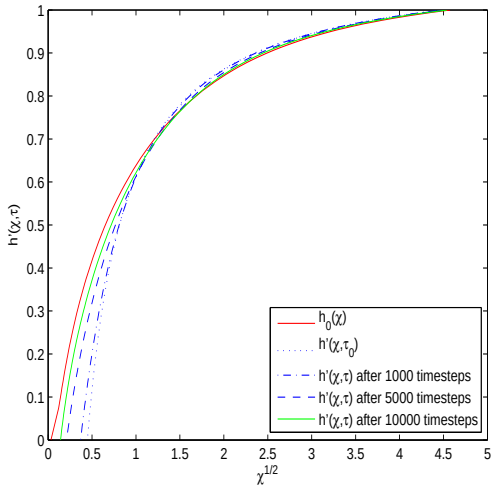


(a) Stable solution. $\Gamma = 0.4$, $\lambda = 10$, $\Delta\tau = 10^{-4}$.

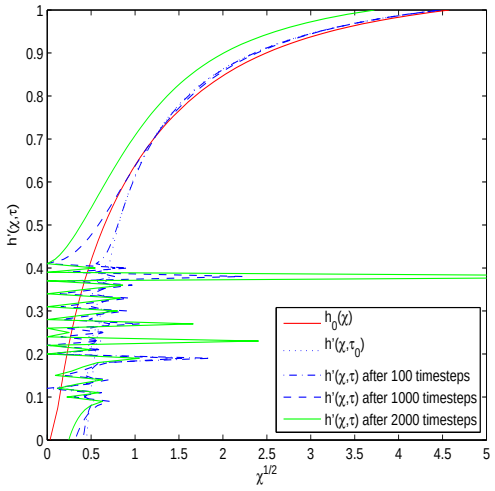


(b) Unstable solution. $\Gamma = 0.4$, $\lambda = 10$, $\Delta\tau = 5 \times 10^{-4}$.

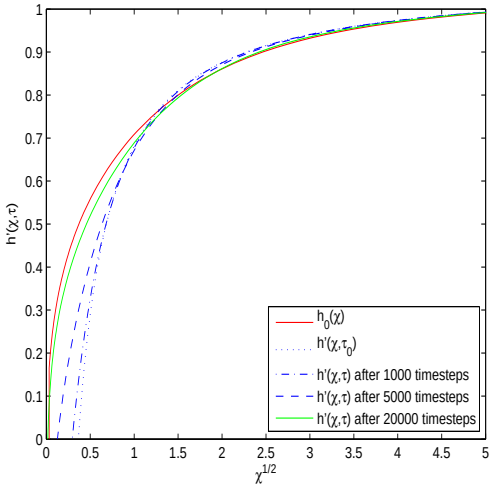


(c) Stable solution. $\Gamma = 0.6$, $\lambda = 15$, $\Delta\tau = 5 \times 10^{-5}$.

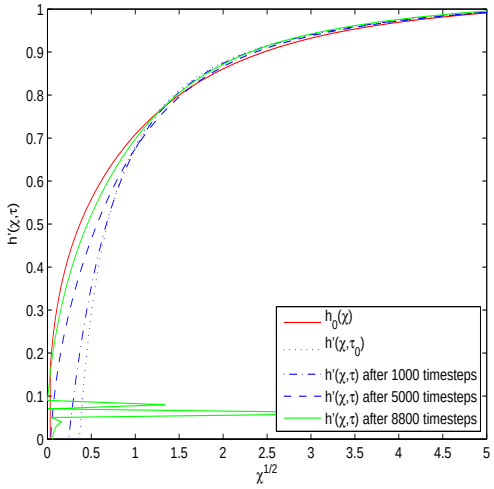


(d) Unstable solution. $\Gamma = 0.6$, $\lambda = 15$, $\Delta\tau = 10^{-4}$.

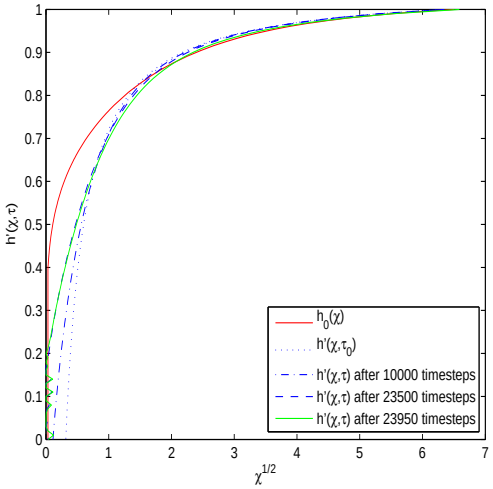


(e) Unstable solution. $\Gamma = 1$, $\lambda = 20$, $\Delta\tau = 10^{-5}$.

# Chapter 6

# Summary and Conclusions

In this thesis, we have studied the stability of the analytical model of Nordbotten and Celia (2006b) for injection of $CO_2$ into confined aquifers. A derivation of this model was given in Chapter 3. By using dimensional analysis, the model was transformed to dimensionless form. The resulting PDE for the vertical interface location in dimensionless form, $h'(\eta, \tau)$, depended on the two dimensionless parameters $\Gamma$ and $\lambda$, defined in (3.9). Here $\eta$ represents dimensionless radial distance from the injection well, while $\tau$ is dimensionless time. A coordinate transformation, $\chi = \frac{\eta^2}{\tau}$, was introduced to reduce the PDE to an ODE for the similarity variable $\chi$. However, in general this transformation will lead to another non-linear PDE for $h' = h'(\chi, \tau)$. For the case of self-similarity, the solution to the new problem should approach a steady-state solution $h' = h_0(\chi)$ for large times $\tau$. In practice this means that the steady-state solution should be stable with respect to perturbations.

In Chapter 4 and 5, the stability of this time-dependent equation was investigated, using analytical and numerical methods. The aim of this investigation was to determine a parameter domain for $\Gamma$ and $\lambda$, in which stability was ensured. In Nordbotten and Celia (2006b) it was proved that the stationary solution was stable for $\Gamma < \Gamma_c(\lambda)$. However, the value of $\Gamma_c$ turned out to be small, as compared to realistic values of $\Gamma$. Since $\Gamma \sim \frac{1}{Q_{\text{well}}}$ (see (3.9)), this shows that the problem becomes more stable for high injection rates.

To extend the analysis of Nordbotten and Celia (2006b), we considered a linear stability analysis of the model equation in Chapter 4. When linearising the time-dependent equation, a function $C = C(\chi)$ appeared in the new equation. We could then show linear stability for the case of $C(\chi) < 0$. However, we were only able to prove that $C(\chi)$ was negative for the boundary points, defined by $h_0(\chi) = 0$ and $h_0(\chi) = 1$.

In Chapter 5 we investigated this problem further, using numerical tools. Numerical experiments indicated that $C(\chi)$ should be negative for all values of $\Gamma > 0$ and $\lambda > 1$. In addition to testing the linear stability numerically, we also investigated the time behaviour of the full mathematical model numerically. From Chapter 4 we obtained an analytical solution $h_0(\chi)$, for the special case of $\Gamma = 0$. This expression was used as an initial condition

for the non-linear time-dependent problem. Numerically, we were able to show that the solution to the time-dependent non-linear equation would approach the stationary solution for $\Gamma < 2 \times \Gamma_c$, where $\Gamma_c$ is the value given by Nordbotten and Celia (2006b) (see (B.8)). However, this results would depend on the size of the time step and various other factors. Thus, no general conclusions can be made.

For small injection rates, $Q_{\text{well}}$, and conversely large $\Gamma$, density forces will be more dominant, and a larger fraction of the injected $CO_2$ will flow on top of the water phase. This results in a steeper interface near the injection well ($\chi = 0$), as shown in Figure 5.1. In our numerical experiments, we observed oscillations in the computed solutions, in this case. These appeared on the steeper part of the interface, when $h'(\chi, \tau) \to 1$ (see Figure 5.7(b), 5.7(d) and 5.7(e)). Whether this is related to the stability of the model is not clear.

# Appendix A

# The Second Derivative of $h_0(\chi)$

We want to derive an expression for the second derivative of $h_0(\chi)$ at the boundary, $\chi_0$ and $\chi_1$. The stationary equation, (4.1), degenerates at the boundary, where $h_0(\chi_0) = 0$ and $h_0(\chi_1) = 1$. Thus, we lose the second derivative term. When we want to derive an expression for the second derivative at the boundary, we will have to differentiate the entire equation first. That is,

$$
\begin{aligned}
&1 + \frac{4\lambda(\lambda-1)\frac{\mathrm{d}h_0}{\mathrm{d}\chi}}{[1+(\lambda-1)h_0]^3} - 4\Gamma\lambda^2\frac{h_0\frac{\mathrm{d}h_0}{\mathrm{d}\chi} + \chi\left(\frac{\mathrm{d}h}{\mathrm{d}\chi}\right)^2 + \chi h_0\frac{\mathrm{d}^2h_0}{\mathrm{d}\chi^2}}{[1+(\lambda-1)h_0]^2} \\
&+ 8\Gamma\lambda^2(\lambda-1)\frac{\chi h_0\left(\frac{\mathrm{d}h_0}{\mathrm{d}\chi}\right)^2}{[1+(\lambda-1)h_0]^3} + 4\Gamma\lambda\frac{(1-h_0)\frac{\mathrm{d}h_0}{\mathrm{d}\chi} - h_0\frac{\mathrm{d}h_0}{\mathrm{d}\chi}}{[1+(\lambda-1)h_0]} - 4\Gamma\lambda(\lambda-1)\frac{h_0(1-h_0)\frac{\mathrm{d}h_0}{\mathrm{d}\chi}}{[1+(\lambda-1)h_0]^2} \\
&\quad + 4\Gamma\lambda\frac{(1-h_0)\frac{\mathrm{d}h_0}{\mathrm{d}\chi} - \chi\left(\frac{\mathrm{d}h_0}{\mathrm{d}\chi}\right)^2 + \chi(1-h_0)\frac{\mathrm{d}^2h_0}{\mathrm{d}\chi^2}}{[1+(\lambda-1)h_0]} - 4\Gamma\lambda(\lambda-1)\frac{\chi(1-h_0)\left(\frac{\mathrm{d}h_0}{\mathrm{d}\chi}\right)^2}{[1+(\lambda-1)h_0]^2} \\
&\quad + 4\Gamma\lambda\frac{(1-h_0)h_0\frac{\mathrm{d}^2h_0}{\mathrm{d}\chi^2}\left(\frac{\mathrm{d}h_0}{\mathrm{d}\chi}\right)^{-1} - \chi h_0\frac{\mathrm{d}^2h_0}{\mathrm{d}\chi^2} + \chi(1-h_0)\frac{\mathrm{d}^2h_0}{\mathrm{d}\chi^2} + \chi h_0(1-h_0)\frac{\mathrm{d}^3h_0}{\mathrm{d}\chi^3}\left(\frac{\mathrm{d}h_0}{\mathrm{d}\chi}\right)^{-1}}{[1+(\lambda-1)h_0]} \\
&\quad - 4\Gamma\lambda\frac{\chi h_0(1-h_0)\left(\frac{\mathrm{d}^2h_0}{\mathrm{d}\chi^2}\right)^2\left(\frac{\mathrm{d}h_0}{\mathrm{d}\chi}\right)^{-2}}{[1+(\lambda-1)h_0]} - 4\Gamma\lambda(\lambda-1)\frac{\chi h_0(1-h_0)\frac{\mathrm{d}^2h_0}{\mathrm{d}\chi^2}}{[1+(\lambda-1)h_0]^2} = 0\,. \quad \text{(A.1)}
\end{aligned}
$$

Substituting $h_0(\chi) = 0$ in the equation above, we obtain

$$
\begin{aligned}
&1 + 4\lambda(\lambda-1)\frac{\mathrm{d}h_0}{\mathrm{d}\chi} - 4\Gamma\lambda^2\chi\left(\frac{\mathrm{d}h_0}{\mathrm{d}\chi}\right)^2 + 4\Gamma\lambda\frac{\mathrm{d}h_0}{\mathrm{d}\chi} + 4\Gamma\lambda\frac{\mathrm{d}h_0}{\mathrm{d}\chi} \\
&\qquad - 4\Gamma\lambda\chi\left(\frac{\mathrm{d}h_0}{\mathrm{d}\chi}\right)^2 + 4\Gamma\lambda\chi\frac{\mathrm{d}^2h_0}{\mathrm{d}\chi^2} - 4\Gamma\lambda(\lambda-1)\chi\left(\frac{\mathrm{d}h_0}{\mathrm{d}\chi}\right)^2 + 4\Gamma\lambda\chi\frac{\mathrm{d}^2h_0}{\mathrm{d}\chi^2} = 0\,,
\end{aligned}
$$

which leads to the expression

$$\left.\frac{\mathrm{d}^2 h_0}{\mathrm{d}\chi^2}\right|_{h_0=0} = \lambda \left(\left.\frac{\mathrm{d}h_0}{\mathrm{d}\chi}\right|_{h_0=0}\right)^2 - \frac{2\Gamma+\lambda-1}{2\Gamma\chi_0}\left.\frac{\mathrm{d}h_0}{\mathrm{d}\chi}\right|_{h_0=0} - \frac{1}{8\Gamma\lambda\chi_0}\,. \tag{A.2}$$

When substituting $h_0(\chi) = 1$ in Equation (A.1), we obtain

$$\begin{aligned} 1 + \frac{4(\lambda-1)}{\lambda^2}\frac{\mathrm{d}h_0}{\mathrm{d}\chi} - 4\Gamma\frac{\mathrm{d}h_0}{\mathrm{d}\chi} - 4\Gamma\chi_1\left(\frac{\mathrm{d}h_0}{\mathrm{d}\chi}\right)^2 - 4\Gamma\chi_1\frac{\mathrm{d}^2 h_0}{\mathrm{d}\chi^2} \\ + \frac{8\Gamma(\lambda-1)}{\lambda}\chi_1\left(\frac{\mathrm{d}h_0}{\mathrm{d}\chi}\right)^2 - 4\Gamma\frac{\mathrm{d}h_0}{\mathrm{d}\chi} - 4\Gamma\chi_1\left(\frac{\mathrm{d}h_0}{\mathrm{d}\chi}\right)^2 - 4\Gamma\chi_1\frac{\mathrm{d}^2 h_0}{\mathrm{d}\chi^2} = 0\,. \end{aligned}$$

This implies,

$$\left.\frac{\mathrm{d}^2 h_0}{\mathrm{d}\chi^2}\right|_{h_0=1} = -\frac{1}{\lambda}\left(\left.\frac{\mathrm{d}h_0}{\mathrm{d}\chi}\right|_{h_0=1}\right)^2 - \left(\frac{1}{\chi_1} - \frac{\lambda-1}{2\Gamma\lambda^2\chi_1}\right)\left.\frac{\mathrm{d}h_0}{\mathrm{d}\chi}\right|_{h_0=1} + \frac{1}{8\Gamma\chi_1}\,. \tag{A.3}$$

# Appendix B

# The Non-Linear Stability Analysis

We will here reproduce the non-linear stability proof of Nordbotten and Celia (2006b). This shows that the solution $h'(\chi)$ of the stationary equation, (3.14), will be an intermediate asymptotic of the solution, $h'(\chi,\tau)$ of (3.13). To ease the presentation, we will use the notation $h'(\chi,\tau) = h$ and $h(\chi) = h_0$.

We assume the interfaces $h$ and $h_0$ as monotone, such that for all $\chi$ and $\tau$

$$\frac{\partial h}{\partial \chi} < 0 \quad \text{and} \quad \frac{\mathrm{d}h_0}{\mathrm{d}\chi} < 0\,. \tag{B.1}$$

Thus, we can use the inverse function theorem (Apostol 1969), and define the inverse function

$$\chi'(\chi) = h^{-1}(h_0(\chi))\,.$$

This function will then relate $\chi'$ to $\chi$, as the values where, $h(\chi') = h(\chi)$. Further we define,

$$\chi_m = \{\chi : |\chi'(\chi_m) - \chi_m| \geq |\chi'(\chi) - \chi|\}\,.$$

Then for $0 < h(\chi'(\chi_m)) < 1$ and $0 < h_0(\chi_m) < 1$, we will have the properties of:

$$\begin{aligned} \frac{\mathrm{d}\chi'}{\mathrm{d}\chi} &= 1\,, \\ \left.\frac{\partial h}{\partial \chi}\right|_{\chi'(\chi_m)} &= \left.\frac{\mathrm{d}h_0}{\mathrm{d}\chi}\right|_{\chi_m}\,, \\ \mathrm{sign}\left(\left.\frac{\partial^2 h}{\partial \chi^2}\right|_{\chi'(\chi_m)} - \left.\frac{\mathrm{d}^2 h_0}{\mathrm{d}^2\chi^2}\right|_{\chi_m}\right) &= -\mathrm{sign}(\chi'(\chi_m) - \chi_m)\,. \end{aligned} \tag{B.2}$$

By subtracting Equation (3.14) from Equation (3.13) we obtain

$$\begin{aligned}\tau\frac{\partial h}{\partial\tau}\Big|_{\chi'(\chi_m)}\left(\frac{\mathrm{d}h_0}{\mathrm{d}\chi}\Big|_{\chi_m}\right)^{-1} &= \{\chi'(\chi_m)-\chi_m\}\Bigg(1-\frac{4\Gamma\lambda^2h_0(\chi_m)}{[1+(\lambda-1)h_0(\chi_m)]^2}\frac{\mathrm{d}h_0}{\mathrm{d}\chi}\Big|_{\chi_m}\\ &\quad+\frac{4\Gamma\lambda(1-h_0(\chi_m))}{1+(\lambda-1)h_0(\chi_m)}\frac{\mathrm{d}h_0}{\mathrm{d}\chi}\Big|_{\chi_m}\Bigg)\\ &\quad+\frac{4\Gamma\lambda h_0(\chi_m)(1-h_0(\chi_m))}{1+(\lambda-1)h_0(\chi_m)}\left(\frac{\mathrm{d}h_0}{\mathrm{d}\chi}\Big|_{\chi_m}\right)^{-1}\\ &\quad\times\left\{\chi'(\chi_m)\frac{\partial^2h}{\partial\chi^2}\Big|_{\chi'(\chi_m)}-\chi_m\frac{\mathrm{d}^2h_0}{\mathrm{d}\chi^2}\Big|_{\chi_m}\right\}.\end{aligned}$$

This further implies

$$\frac{\partial h}{\partial\tau}\Big|_{\chi'(\chi_m)}\left(\frac{\mathrm{d}h_0}{\mathrm{d}\chi}\Big|_{\chi_m}\right)^{-1}=\frac{c_1}{\tau}\{\chi'(\chi_m)-\chi_m\}+\frac{c_2}{\tau}\left\{\frac{\partial^2h}{\partial\chi^2}\Big|_{\chi'(\chi_m)}-\frac{\mathrm{d}^2h_0}{\mathrm{d}\chi^2}\Big|_{\chi_m}\right\},\qquad\text{(B.3)}$$

where $c_1$ and $c_2$ are defined as

$$\begin{aligned}c_1=1-\Gamma\Bigg[&\frac{4\lambda}{1+(\lambda-1)h_0(\chi_m)}\left(\frac{\lambda h_0(\chi_m)}{1+(\lambda-1)h_0(\chi_m)}-(1-h_0(\chi_m))\right)\frac{\mathrm{d}h_0}{\mathrm{d}\chi}\Big|_{\chi_m}\\ &-\frac{4\lambda h_0(\chi_m)(1-h_0(\chi_m))}{1+(\lambda-1)h_0(\chi_m)}\left(\frac{\mathrm{d}h_0}{\mathrm{d}\chi}\Big|_{\chi_m}\right)^{-1}\frac{\mathrm{d}^2h_0}{\mathrm{d}\chi^2}\Big|_{\chi_m}\Bigg],\end{aligned}\qquad\text{(B.4a)}$$

$$c_2=\chi'(\chi_m)\frac{4\Gamma\lambda h_0(\chi_m)(1-h_0(\chi_m))}{1+(\lambda-1)h_0(\chi_m)}\left(\frac{\mathrm{d}h_0}{\mathrm{d}\chi}\Big|_{\chi_m}\right)^{-1}.\qquad\text{(B.4b)}$$

We will consider $0<\Gamma<\infty$ and $1<\lambda<\infty$. Thus, we see from (B.4a) that if $\frac{\mathrm{d}h_0}{\mathrm{d}\chi}$ and $\frac{\mathrm{d}^2h_0}{\mathrm{d}\chi^2}$ are bounded, $c_1>0$ when $\Gamma<\Gamma_c$. The value of $\Gamma_c$ will further depend on $\lambda$, $h_0$ and $\frac{\mathrm{d}h_0}{\mathrm{d}\chi}$. By assumption (B.1), we further see from (B.4b) that $c_2<0$ for all positive values of $\chi$ and $\chi'$.

Considering $\Gamma<\Gamma_c$. From (B.3) we thus obtain

$$\begin{aligned}\frac{\partial}{\partial\tau}(\chi'(\chi_m)-\chi_m) &= -\frac{\partial h}{\partial\tau}\Big|_{\chi'(\chi_m)}\left(\frac{\mathrm{d}h_0}{\mathrm{d}\chi}\Big|_{\chi_m}\right)^{-1}\\ &= -\frac{c_1}{\tau}(\chi'(\chi_m)-\chi_m)-\frac{c_2}{\tau}\left(\frac{\partial^2h}{\partial\chi^2}\Big|_{\chi'(\chi_m)}-\frac{\mathrm{d}^2h_0}{\mathrm{d}\chi^2}\Big|_{\chi_m}\right).\end{aligned}\qquad\text{(B.5)}$$

This equation, together with the third property of (B.2), shows that the maximum difference between $\chi'$ and $\chi$ will strictly decreasing, when $\chi_m$ is not at the boundary.

When $\chi_m$ is at the top boundary, we have $h(\chi_m) = 0$. We again subtract Equation (3.14) from Equation (3.13). This yields,

$$\frac{\partial h}{\partial \tau}\bigg|_{\chi_m} \left( \frac{\mathrm{d}h_0}{\mathrm{d}\chi}\bigg|_{\chi_m} \right)^{-1} = \frac{1}{\tau}(\chi'(\chi_m) - \chi_m) + \frac{4\Gamma\lambda}{\tau} \left( \chi'(\chi_m) \frac{\partial h}{\partial \chi}\bigg|_{\chi'(\chi_m)} - \chi_m \frac{\mathrm{d}h_0}{\mathrm{d}\chi}\bigg|_{\chi_m} \right) .$$

When $\chi_m$ is the local maximum at the top boundary, the derivative of $h$ and $h_0$ must satisfy

$$\operatorname{sign}\left( \frac{\partial h}{\partial \chi} - \frac{\mathrm{d}h_0}{\mathrm{d}\chi} \right) = \operatorname{sign}(\chi'(\chi_m) - \chi_m) .$$

Thus, the equivalent expression to (B.5), when considering $\chi_m$ at the top boundary is,

$$\frac{\partial}{\partial \tau}\chi'(\chi_m) > -\frac{1}{\tau} \left( 1 + 4\Gamma\lambda \frac{\mathrm{d}h_0}{\mathrm{d}\chi}\bigg|_{\chi_m} \right) [\chi'(\chi_m) - \chi_m] \quad \text{when} \quad \chi'(\chi_m) < \chi_m , \tag{B.6a}$$

$$\frac{\partial}{\partial \tau}\chi'(\chi_m) < -\frac{1}{\tau} \left( 1 + 4\Gamma\lambda \frac{\mathrm{d}h_0}{\mathrm{d}\chi}\bigg|_{\chi_m} \right) [\chi'(\chi_m) - \chi_m] \quad \text{when} \quad \chi'(\chi_m) > \chi_m . \tag{B.6b}$$

Considering $\chi_m$ as the local maximum at the bottom boundary, the derivative of $h$ and $h_0$ will have to satisfy

$$\operatorname{sign}\left( \frac{\partial h}{\partial \chi} - \frac{\mathrm{d}h_0}{\mathrm{d}\chi} \right) = -\operatorname{sign}(\chi'(\chi_m) - \chi_m) ,$$

and we get

$$\frac{\partial}{\partial \tau}\chi'(\chi_m) > -\frac{1}{\tau} \left( 1 - 4\Gamma\lambda \frac{\mathrm{d}h_0}{\mathrm{d}\chi}\bigg|_{\chi_m} \right) [\chi'(\chi_m) - \chi_m] \quad \text{when} \quad \chi'(\chi_m) < \chi_m , \tag{B.7a}$$

$$\frac{\partial}{\partial \tau}\chi'(\chi_m) < -\frac{1}{\tau} \left( 1 - 4\Gamma\lambda \frac{\mathrm{d}h_0}{\mathrm{d}\chi}\bigg|_{\chi_m} \right) [\chi'(\chi_m) - \chi_m] \quad \text{when} \quad \chi'(\chi_m) > \chi_m . \tag{B.7b}$$

From (B.6a)-(B.6b) and (B.7a)-(B.7b), together with (B.5), we observe that $|\chi' - \chi|$ is strictly decreasing for $\Gamma < \Gamma_c$. Thus, we have stability for the case of $\Gamma < \Gamma_c$. That is,

$$1-\Gamma\Bigg[\frac{4\lambda}{1+(\lambda-1)h_0(\chi_m)}\left(\frac{\lambda h_0(\chi_m)}{1+(\lambda-1)h_0(\chi_m)}-(1-h_0(\chi_m))\right)\frac{\mathrm{d}h_0}{\mathrm{d}\chi}\bigg|_{\chi_m} - \frac{4\lambda h_0(\chi_m)(1-h_0(\chi_m))}{1+(\lambda-1)h_0(\chi_m)}\left(\frac{\mathrm{d}h_0}{\mathrm{d}\chi}\bigg|_{\chi_m}\right)^{-1}\frac{\mathrm{d}^2h_0}{\mathrm{d}\chi^2}\bigg|_{\chi_m}\Bigg]>0\,. \quad \text{(B.8)}$$

# References


Apostol, T. M. (1969). *Calculus. Multi-Variable Calculus and Linear Algebra, with Applications to Differential Equations and Probability* (2 ed.), Volume 2. JOHN WILEY & SONS.

Bachu, S., J. M. Nordbotten, and M. A. Celia (2004). Evaluation of the spread of acid-gas plumes injected in deep saline aquifers in western Canada as an analogue for $CO_2$ injection into continental sedimentary basins. In *In Proceeding of the 7th International Conference on Greenhouse Gas Control Technologies, Vancouver, BC, Canada.*

Barenblatt, G. I. (1996). *Scaling, self-similarity, and intermediate asymptotics*. Cambridge University Press.

Cheney, W. and D. Kincaid (2002). *Numerical Analysis, Mathematics of Scientific Computing*. BROOKS/COLE.

Etheridge, D. M., L. P. Steele, R. L. Langenfelds, R. J. Francey, J. M. Barnola, and V. I. Morgan (1998). Historical $CO_2$ records from the Law Dome DE08, DE08-2 and DSS ice cores. *TRENDS: A Compendium of Data on Global Change*.

Evans, L. C. (1998). *Partial Differential Equations*, Volume 19. American Mathematical Society.

Hairer, E., S. P. Nørsett, and G. Wanner (1987). *Solving Ordinary Differential Equations I. Nonstiff Problems*, Chapter 2, pp. 165–175. Springer-Verlag.

Hubbert, M. K. (1956). Darcy's Law and The Field Equations of The Flow of Underground Fluids. *Journal of Petroleum Technology* (104), 24–59.

Hyne, N. J. (1984). *Geology for Petroleum Exploration, Drilling, and Production*, Chapter 13, pp. 144–151. McGraw-Hill book company.

IPCC (2005). IPCC: Special Report on Carbondioxide Capture and Storage. Prepared by Working Group III of the Intergovernmental Panel on Climate Change. Technical report, IPCC.

Keeling, C. D. and T. P. Whorf (2005). Atmospheric $CO_2$ records from sites in the SIO air sampling network. *TRENDS: A Compendium of Data on Global Change*.

Lindeberg, E. (2003). The quality of a $CO_2$ repository: what is the sufficient retention time of $CO_2$ stored underground. In J. Gale and Y. Kaya (Eds.), *Proceeding of the 6th*

*International Greenhouse Gas Control Technologies Kyoto*, Volume 1, pp. 255–260.

Nordbotten, J. M. and M. A. Celia (2006a). Analysis of plume extent using analytical solutions for $CO_2$ storage. In *Proceedings of the 16th conference on Computational Methods in Water Resources*.

Nordbotten, J. M. and M. A. Celia (2006b). Similarity solutions for fluid injection into confined aquifers. *Journal of Fluid Mechanics 561*, 307–327.

Pettersen, Ø. (1990). Grunnkurs i Reservoarmekanikk.

Solomon, S., D. Qin, M. Manning, Z. Chen, M. Marquis, K. B. Averyt, M. Tignor, and H. L. Miller (2007). Climate Change 2007: The Physical Science Basis. Contribution of Working Group I to the Fourth Assessment Report of the Intergovernmental Panel on Climate Change. Technical report, IPCC.